Journal of Physiology (1995), **485.2**, *pp.* 383–402

Ca^{2+}-permeable AMPA and NMDA receptor channels in basket cells of rat hippocampal dentate gyrus

D.-S. Koh, J. R. P. Geiger, P. Jonas and B. Sakmann *

Max-Planck-Institut für medizinische Forschung, Abteilung Zellphysiologie, Jahnstraße 29, 69120 Heidelberg, Germany

1. Glutamate receptor (GluR) channels were studied in basket cells in the dentate gyrus of rat hippocampal slices. Basket cells were identified by their location, dendritic morphology and high frequency of action potentials generated during sustained current injection.

2. Dual-component currents were activated by fast application of glutamate to outside-out membrane patches isolated from basket cell somata (10 μM glycine, no external Mg^{2+}). The fast component was selectively blocked by 6-cyano-7-nitroquinoxaline-2,3-dione (CNQX), the slow component by D-2-amino-5-phosphonopentanoic acid (D-AP5). This suggests that the two components were mediated by α-amino-3-hydroxy-5-methyl-4-isoxazolepropionate receptor (AMPAR)/kainate receptor and *N*-methyl-D-aspartate receptor (NMDAR) channels, respectively. The mean ratio of the peak current of the NMDAR component to that of the AMPAR/kainate receptor component was 0·22 (1 ms pulses of 10 mM glutamate).

3. The AMPAR/kainate receptor component, which was studied in isolation in the presence of D-AP5, was identified as AMPAR mediated on the basis of the preferential activation by AMPA as compared with kainate, the weak desensitization of kainate-activated currents, the cross-desensitization between AMPA and kainate, and the reduction of desensitization by cyclothiazide.

4. Deactivation of basket cell AMPARs following 1 ms pulses of glutamate occurred with a time constant (τ) of 1·2 ± 0·1 ms (mean ± S.E.M.). During 100 ms glutamate pulses, AMPARs desensitized with a τ of 3·7 ± 0·2 ms.

5. The peak current–voltage (*I–V*) relation of AMPAR-mediated currents in Na^+-rich extracellular solution showed a reversal potential of −4·0 ± 2·6 mV and was characterized by a doubly rectifying shape. The conductance of single AMPAR channels was estimated as 22·6 ± 1·6 pS using non-stationary fluctuation analysis. AMPARs expressed in hippocampal basket cells were highly Ca^{2+} permeable ($P_{Ca}/P_K = 1·79$).

6. NMDARs in hippocampal basket cells were studied in isolation in the presence of CNQX. Deactivation of NMDARs activated by glutamate pulses occurred bi-exponentially with mean τ values of 266 ± 23 ms (76%) and 2620 ± 383 ms (24%).

7. The peak *I–V* relation of the NMDAR-mediated component in Na^+-rich extracellular solution showed a reversal potential of 1·5 ± 0·6 mV and a region of negative slope at negative membrane potentials in the presence of external Mg^{2+}, due to voltage-dependent block by these ions. The conductance of single NMDAR channels in the main open state was 50·2 ± 1·8 pS. NMDARs in hippocampal basket cells were highly permeable to Ca^{2+} ($P_{Ca}/P_K = 6·68$).

8. AMPARs in hippocampal basket cells are characterized by about threefold faster kinetics and twentyfold higher Ca^{2+} permeability than AMPARs in hippocampal granule or pyramidal cells. Simulations show that the Ca^{2+} influx through basket cell AMPARs is comparable to that through NMDARs at negative membrane potentials with physiological concentrations of Ca^{2+} and Mg^{2+}. This suggests a dual pathway of synaptically mediated Ca^{2+} entry into interneurones.

* To whom correspondence should be addressed.

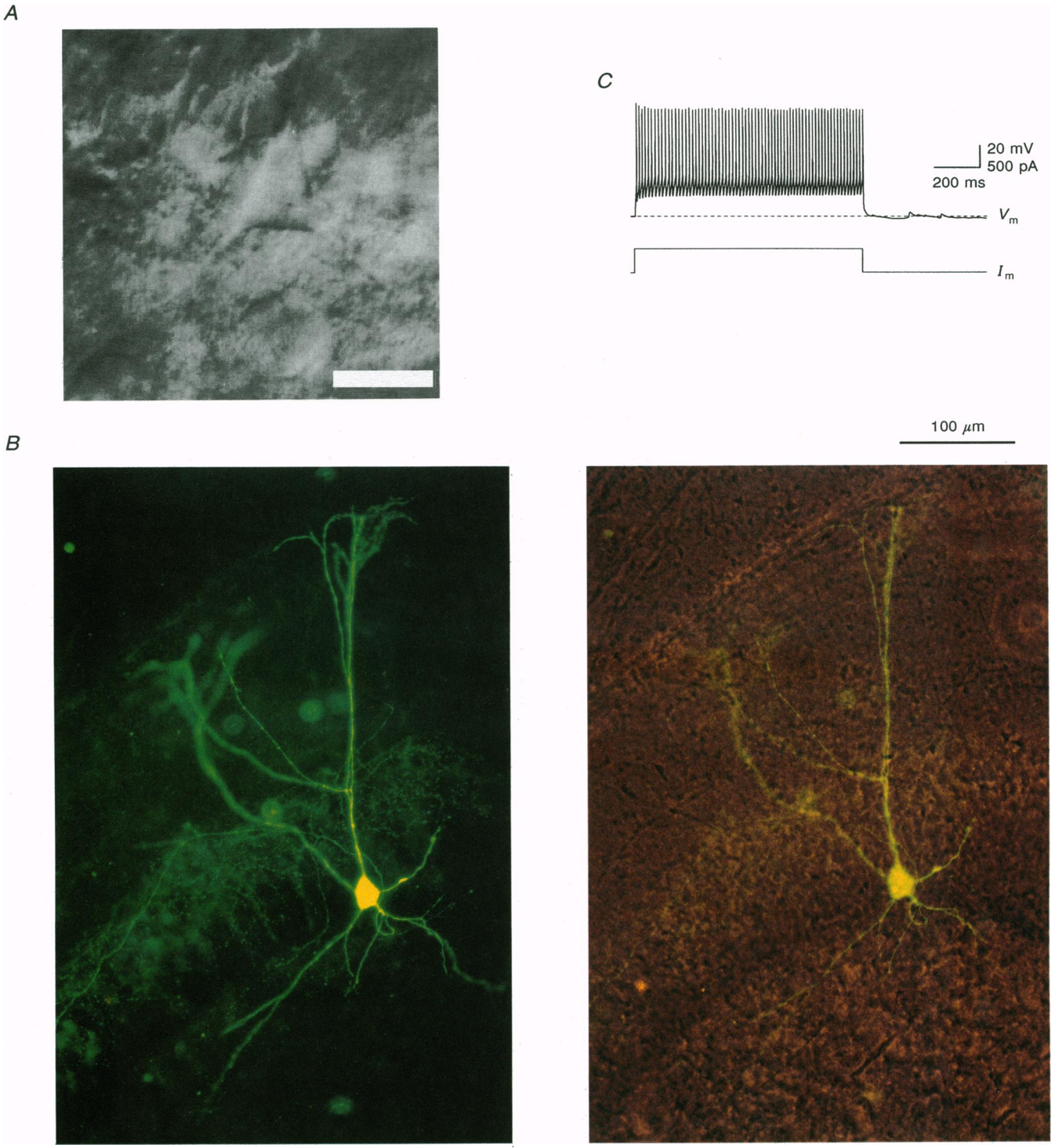

Figure 1. Identification of dentate gyrus basket cells in living brain slices from rat hippocampus using IR-DIC videomicroscopy

A, photomicrograph of a video-enhanced, IR-DIC image of a hippocampal dentate gyrus basket cell with cell body of pyramidal shape. The border between the granule cell layer and the hilus is visible in the middle of the photomicrograph. The triangular basket cell soma is located at the border between the two layers. A single apical dendrite is extending 'upwards' through the granule cell layer; two basal dendrites are extending 'downwards' towards the hilar region. Scale bar, 20 μm. *B*, fluorescence photomicrograph of a different basket cell filled with biocytin and stained using fluorescein–avidin. Left panel, UV epiillumination; right panel, UV epiillumination combined with visible light transillumination. The hilus is in the lower part, the granule cell layer is visible as a curved band in the middle of the image. Note that

Glutamate, the major excitatory neurotransmitter in the mammalian central nervous system (CNS), mediates synaptic transmission by acting on α-amino-3-hydroxy-5-methyl-4-isoxazolepropionate (AMPA)- or kainate-type and *N*-methyl-D-aspartate (NMDA)-type glutamate receptor (GluR) channels (Wisden & Seeburg, 1993). At many synapses AMPA/kainate and NMDA receptors are colocalized and coactivated by synaptically released glutamate (Jonas & Spruston, 1994). Determining the Ca^{2+} permeability of these receptors is important for the understanding of excitatory synaptic transmission in the CNS, since Ca^{2+} is an intracellular second messenger and triggers long-lasting changes in synaptic efficacy, e.g. long-term potentiation (LTP; Bliss & Collingridge, 1993). AMPA/kainate-type GluRs are thought to be weakly permeable to Ca^{2+}, whereas the Ca^{2+} permeability of NMDA-type GluRs is high (Mayer & Westbrook, 1987; Ascher & Nowak, 1988; Iino, Ozawa & Tsuzuki, 1990; Jonas & Sakmann, 1992; Colquhoun, Jonas & Sakmann, 1992; Wyllie & Cull-Candy, 1994; Spruston, Jonas & Sakmann, 1995).

Recent studies, however, suggest functional diversity of AMPARs expressed in different types of neurones in the CNS with respect to their Ca^{2+} permeability. In cell culture, the majority of hippocampal neurones express AMPARs with low Ca^{2+} permeability, but subsets of cells, presumably GABAergic interneurones, express AMPARs with high Ca^{2+} permeability (Iino *et al.* 1990; Bochet *et al.* 1994; Lerma, Morales, Ibarz & Somohano, 1994). AMPARs expressed in hippocampal and neocortical principal (e.g. pyramidal) neurones in brain slices are characterized by low Ca^{2+} permeability (Colquhoun *et al.* 1992; Jonas, Racca, Sakmann, Seeburg & Monyer, 1994; Spruston *et al.* 1995), whereas AMPAR channels with higher Ca^{2+} permeability have been described in non-pyramidal interneurones of neocortex (Jonas *et al.* 1994). In addition, a subset of interneurones in the CA3 subfield of hippocampal slices shows inwardly rectifying steady-state current–voltage (I–V) relations of kainate-activated currents (McBain & Dingledine, 1993), suggesting the expression of Ca^{2+}-permeable AMPAR channels. Heterologously expressed recombinant AMPARs containing the GluR-B subunit in its edited form show low Ca^{2+} permeability, whereas AMPARs lacking this subunit are highly Ca^{2+} permeable (Hollmann, Hartley & Heinemann, 1991; Burnashev, Monyer, Seeburg & Sakmann, 1992; Wisden & Seeburg, 1993). In accordance with these results, the relative abundance of GluR-B mRNA is much higher in neurones expressing Ca^{2+}-impermeable AMPARs than in neurones expressing Ca^{2+}-permeable AMPARs (Bochet *et al.* 1994; Jonas *et al.* 1994). The available data thus raise the possibility that inhibitory interneurones in the CNS specifically express Ca^{2+}-permeable AMPARs, possibly by expressing the GluR-B subunit only at a low level.

To cast more light on the functional properties of GluRs in interneurones, we studied AMPARs and NMDARs in the basket cell of hippocampal dentate gyrus. This cell is typical of inhibitory interneurones in the CNS, mediating recurrent inhibition via mossy fibre collateral innervation as well as feed-forward inhibition through perforant path afferents (Ribak & Seress, 1983; Seress & Ribak, 1983). Normal excitatory innervation of basket cells appears to be critical for the function of the hippocampal circuits. A reduction of excitatory synaptic drive to basket cells has been proposed to be involved in the pathophysiology of epilepsy (the 'dormant basket cell hypothesis'; Sloviter, 1991). Morphological characteristics and action potential pattern allow us to identify basket cells in living brain slices. Fast application of glutamate to membrane patches excised from the cell somata revealed that AMPARs in hippocampal basket cells were functionally distinct from those in principal neurones (Colquhoun *et al.* 1992; Spruston *et al.* 1995), particularly with respect to faster kinetics and higher permeability to Ca^{2+}. The amount of Ca^{2+} entry through AMPARs in hippocampal basket cells appears to be comparable to that flowing through NMDARs during synapse-like coactivation by brief glutamate pulses.

METHODS

Visual identification of basket cells in hippocampal slices

Transverse 200–250 μm-thick hippocampal slices were cut from the brains of 13- to 15-day-old Wistar rats, which were killed by decapitation. Basket cells in the dentate gyrus were visualized using infrared differential interference contrast (IR-DIC) videomicroscopy (Stuart, Dodt & Sakmann, 1993; Fig. 1*A*) utilizing a Newvicon camera (C2400, Hamamatsu, Hamamatsu City, Japan) and an infrared filter (RG9, Schott, Mainz, Germany) mounted on an upright microscope (Axioskop FS, Zeiss, Oberkochen, Germany). To confirm visual identification of cells, a subset of basket cells was filled with biocytin for 30 min in the whole-cell recording configuration (Jonas, Major & Sakmann, 1993). Slices were fixed overnight in 2% paraformaldehyde and

---

the main apical dendrite of the filled basket cell is extending towards the molecular layer and the axonal arbor is located in the external granule cell layer. The cell had sparsely spiny dendrites with varicosities. Scale bar, 100 μm. *C*, impulse pattern in response to sustained current injection (500 pA, 1 s) recorded about 30 s after establishing whole-cell recording. Note lack of adaptation and the high action potential frequency (71 APs s^{-1}). Resting membrane potential was −65 mV; membrane potential was held as −70 mV (dashed line) by injection of a small constant current.

2·5% glutaraldehyde, stained with fluorescein–avidin (Vector Laboratories, Burlingame, CA, USA), and examined using epifluorescence illumination (Fig. 1*B*).

Patch clamp recording and fast application of agonists

Patch pipettes were pulled from borosilicate glass tubing (2·0 mm outer diameter, 0·5 mm wall thickness). When filled with a K^+-rich internal solution, they had a resistance of 2–5 MΩ. For non-stationary fluctuation analysis and single-channel experiments, pipettes were coated with Sylgard (Dow Corning, Midland, MI, USA). Morphologically identified neurones were approached with patch pipettes under visual control while positive pressure was applied to the interior of the patch pipette; no cleaning of the cell somata was performed (Stuart *et al.* 1993). Fast application of agonists to outside-out membrane patches (Franke, Hatt & Dudel, 1987) isolated from cell somata was performed as described (Colquhoun *et al.* 1992). Fast application experiments were started 1–2 min after the patch was excised. The double-barrelled application pipette was fabricated from theta glass tubing (2 mm outer diameter, 0·3 mm wall thickness, 0·12 mm septum, Hilgenberg, Malsfeld, Germany), and the Piezo-electric element used was a P-245.50 (Physik Instrumente, Waldbronn, Germany) operated by a Piezo power switch (P-272.00). The exchange time (20–80%), measured with an open patch pipette during a change between Na^+-rich and 10% Na^+-rich solutions, was 50–150 μs. Agonist pulses were applied to outside-out patches every 3 s for activation of AMPARs and every 10–25 s for activation of NMDARs. Membrane current was recorded with an EPC-7 amplifier (List Electronic, Darmstadt, Germany) and filtered at a bandwidth (−3 dB) of 3 kHz (AMPARs) or 1 kHz (NMDARs) with an 8-pole low-pass Bessel filter. Data were digitized and stored on-line using a VMEbus computer system (Delta series 1147, Motorola, Tempe, AZ, USA). The sampling frequency was twice the filter frequency. All recordings were made at room temperature (around 22 °C). Traces shown in the figures are the means of two to ten single traces, unless otherwise noted. In addition to the experiments on dentate gyrus basket cells, a few Ca^{2+} permeability measurements were also performed on patches isolated from dentate gyrus granule cells. To minimize the washout of cytoplasmic factors, some experiments on basket cell AMPARs were made using perforated vesicles (Levitan & Kramer, 1990). Nystatin (Sigma, St Louis, MO, USA) was dissolved in dimethyl sulphoxide and diluted in internal solution to a final concentration of 120 μg ml^{-1}. The patch pipette was withdrawn after an access resistance of 20–40 MΩ had developed in the cell-attached configuration.

Solutions and drugs

Slices were continuously superfused with physiological extracellular solution containing (mM): 125 NaCl, 25 $NaHCO_3$, 25 glucose, 2·5 KCl, 1·25 NaH_2PO_4, 2 $CaCl_2$, 1 $MgCl_2$, bubbled with 95% O_2–5% CO_2. The Hepes-buffered Na^+-rich external solution used for fast application contained (mM): 135 NaCl, 5·4 KCl, 1·8 $CaCl_2$, 1 $MgCl_2$, 5 Hepes; pH adjusted to 7·2 with NaOH. The 100 mM Ca^{2+}-rich external solution contained (mM): 100 $CaCl_2$, 5 Hepes; pH adjusted to 7·2 with $Ca(OH)_2$; the final Ca^{2+} concentration was 101·25 mM. The 30/10/1·8 mM Ca^{2+} external solutions contained 30/10/1·8 $CaCl_2$, 105/135/147·3 *N*-methyl-D-glucamine (NMG), 5 Hepes; pH adjusted to 7·2 with HCl. The K^+-rich internal solution contained (mM): 140 KCl, 10 EGTA, 2 $MgCl_2$, 2 Na_2ATP, 10 Hepes; pH adjusted to 7·3 with KOH; the final K^+ concentration was about 165 mM. The internal solution for staining with biocytin contained (mM): 13 biocytin, 120 potassium gluconate, 20 KCl, 10 EGTA, 2 $MgCl_2$, 2 Na_2ATP, 10 Hepes; pH adjusted to 7·3 with KOH. The pipette solution for the perforated vesicles contained (mM): 120 KCl, 20 K_2SO_4, 10 EGTA, 2 $MgCl_2$, 2 Na_2ATP, 10 Hepes; pH adjusted to 7·3 with KOH. Dual-component glutamate-activated currents were measured in an external solution to which 10 μM glycine was added and from which Mg^{2+} was omitted (solutions in both barrels of the application pipette). To study AMPARs in isolation, glycine was omitted and 50 μM D-AP5 was added (both barrels). To study NMDARs in isolation, 10 μM glycine and 10 μM CNQX were added (both barrels) and external Mg^{2+} was omitted (unless otherwise mentioned). L-AMPA, CNQX, and D-AP5 were from Tocris Cookson (Bristol, UK), cyclothiazide was from Eli Lilly (Indianapolis, IN, USA), and all other chemicals were from Sigma. Stock solutions of 100 mM glutamate and kainate and 25 mM AMPA were prepared either in distilled water or in the final solution; the pH was adjusted with NaOH, $Ca(OH)_2$, or NMG (free base) depending on the major cation in the final solution. For analysis of the concentration dependence, cyclothiazide was added to the solutions in both barrels of the application system. CNQX and D-AP5, however, were added only to the control barrel solution, because the unbinding of these competitive GluR antagonists is thought to be slow compared with the length of the glutamate pulse used (1 ms; Colquhoun *et al.* 1992).

Analysis

Non-linear least-squares fitting was performed using either a Simplex or a modified Gauss–Newton algorithm. Deactivation and desensitization time constants of the AMPAR-mediated component were determined by fitting the decay phase with a single- or double-exponential function. The time interval used for the fit was 0·3 to about 80 ms after the peak. Rise, deactivation and desensitization time constants of the NMDAR-mediated component were determined either by fitting the decay phase with the sum of two exponentials or by fitting rise and decay with the sum of three exponentials; the fitted range extended to 7 s after the peak. Data points of *I–V* relations were fitted by 4th- or 5th-order polynomials, from which the interpolated reversal potentials were calculated.

Concentration–response curves were fitted with the function:

$$f(c) = 1/[1 + (K/c)^n], \quad (1)$$

where c denotes concentration, K represents either the half-maximal effective concentration (EC_{50}) or the half-maximal inhibitory concentration (IC_{50}), and n denotes the Hill coefficient.

The single-channel conductance of AMPARs was estimated by non-stationary fluctuation analysis of glutamate-activated currents (Jonas *et al.* 1993; Spruston *et al.* 1995). Local variances and means were calculated for ensembles consisting of ten traces each, and the mean variance (σ^2) obtained from five to ten ensembles was plotted against the mean current (I). Data points were fitted with the function:

$$\sigma^2(I) = iI - I^2/N + \sigma_b^2, \quad (2)$$

where i represents the apparent single-channel current, N denotes the number of available channels in the patch, and σ_b^2 is the variance of the background noise. Fluctuation analysis also allowed us to estimate the open probability of channels at the peak as peak current divided by iN. The single-channel current through NMDARs corresponding to the main open state was measured directly by eye using cursors.

Plots of reversal potential (V_{rev}) against activity of external Ca^{2+} (a_{Ca_o}) were fitted using the equation (Lewis, 1979; Iino *et al.* 1990):

$$V_{rev}(a_{Ca_o}) = RT/F \ln\{0{\cdot}5[-1 + \sqrt{((1 + 16\,P_{Ca}/P_K)(a_{Ca_o}/a_{K_i}))}]\}, \quad (3)$$

where P_{Ca}/P_K denotes the relative permeability to Ca^{2+} as compared with K^+, a_{K_i} represents the activity of K^+ in the internal solution, and R, T and F are standard thermodynamic parameters. Ion activity coefficients were estimated by interpolation of tabulated values (Robinson & Stokes, 1965; A. Roth & E. v. Kitzing (Heidelberg), unpublished data) as 0·732 for 165 mM K^+ and 0·515, 0·550, 0565 and 0·571 for 100, 30, 10 and 1·8 mM Ca^{2+}, respectively. The measured reversal potential values reported in the text and Table 1 are not corrected for liquid junction potentials. V_{rev} values used in V_{rev} (a_{Ca_o}) plots (Figs 8*D* and 12*D*), however, were corrected as follows. The junction potential between Na^+-rich external and K^+-rich internal solutions, determined using recording pipettes filled with 3 M KCl solution, was +4·5 mV. The junction potentials between external solutions containing 100, 30, 10 and 1·8 mM Ca^{2+} and Na^+-rich external solution were +5·9, +5·3, +5·2 and +5·1 mV, respectively; reversal potentials measured under these conditions were in total corrected by −10·4, −9·8, −9·7 and −9·6 mV, respectively.

The voltage-dependent block of NMDARs by Mg^{2+} was modelled using Woodhull's theory (Woodhull, 1973) as:

$$I(V) = I_0(V)/[1 + [Mg^{2+}]_o \exp(-\delta zFV/RT)/K_0], \quad (4)$$

where I_0 represents the current in the absence of external Mg^{2+}, $[Mg^{2+}]_o$ is the external Mg^{2+} concentration, K_0 denotes the half-maximal blocking concentration at 0 mV, δ is the apparent electrical distance of the Mg^{2+} binding site from the outside of the membrane and z is the valence of Mg^{2+}.

To simulate the Ca^{2+} influx through AMPARs and NMDARs in physiological conditions, fractional Ca^{2+} currents (P_f) were calculated from permeability ratios according to the Goldman–Hodgkin–Katz (GHK) current equation (Schneggenburger, Zhou, Konnerth & Neher, 1993; Burnashev, Zhou, Neher & Sakmann, 1995), assuming the internal Ca^{2+} concentration to be zero:

$$P_f = 1/\{1 + (P_M/P_{Ca})(a_M/a_{Ca_o})[1 - \exp(-2FV/RT)]/4\}, \quad (5)$$

where P_M denotes the permeability (assumed to be the same for all monovalent cations) and a_M represents the total activity of monovalent cations (assumed to be equal on both sides of the membrane). Simulations were performed using a commercially available software package, Mathematica (Version 2.2, Wolfram Research, Champaign, IL, USA).

All numerical values given denote mean ± standard error of the mean (S.E.M.).

RESULTS

Identification of basket cells in dentate gyrus of hippocampal slices

Putative dentate gyrus basket cells were visually identified in hippocampal brain slices using IR-DIC videomicroscopy (Stuart *et al.* 1993) according to the following criteria (Ribak & Seress, 1983): (1) the location of the somata at the border between the granule cell layer and the polymorphic layer of the hilus, (2) the large diameter of the somata (range about 15–25 μm), and (3) the typical dendritic architecture, with a major apical dendrite extending into the granule cell layer and two or more basal dendrites directed towards the hilar region (Fig. 1*A*). The neurones selected resembled pyramidal or fusiform basket cells according to the classification of Ribak & Seress (1983).

To elucidate additional anatomical details, the dendritic and axonal architecture of fifteen cells was investigated by intracellular loading with biocytin and staining using fluorescein-conjugated avidin (Fig. 1*B*). The dendrites of all cells were aspiny or sparsely spiny and showed varicosities, a feature that has been suggested to be typical for inhibitory interneurones in the CNS (Ribak & Seress, 1983). The majority of cells (14 of 15) were characterized by an axon projecting to the granule cell layer and were thus tentatively identified as basket cells, although it was not possible to distinguish whether the axon terminals were formed on somata or axon initial segments of the postsynaptic granule cells using light microscopy (Han, Buhl, Lörinczi & Somogyi, 1993). In one neurone, the axon projected to the molecular layer; this cell resembled the anatomical characteristics of the 'MOLAX' cell type described by Soriano & Frotscher (1993). Based on the target region of the axon in the majority of cases, the cells were designated as basket cells.

Inhibitory interneurones are thought to be characterized by high-frequency impulse activity during sustained current injection (Han *et al.* 1993; Hestrin, 1993; Jonas *et al.* 1994). We therefore measured resting potential and action potential pattern of every cell in the current clamp recording configuration before a membrane patch was isolated. Typical resting potentials of basket cells after breaking the patch membrane were about −65 mV. During sustained 1 s depolarizing current pulses (100–700 pA), the majority of cells (about 70%) showed continuous fast spiking at a high frequency up to 100 Hz (Fig. 1*C*). The remaining cells (30%) either exhibited repetitive activity which ceased and then restarted or showed impulse activity which ceased after a few action potentials. These results show that the majority of basket cells were characterized by a high-frequency action potential pattern, but that some heterogeneity in discharge characteristics exists. No differences were noted in the properties of AMPAR and NMDAR channels in outside-out patches (see below) between basket cells showing different action potential patterns.

Dual-component glutamate-activated current in basket cell patches

The functional properties of GluR channels in basket cells of hippocampal dentate gyrus were characterized using fast application of glutamate to membrane patches isolated from

the somata of these neurones (Colquhoun *et al.* 1992). Initial experiments were performed in the presence of 10 μM glycine and in the absence of external Mg^{2+} to activate both AMPA/kainate- and NMDA-type GluRs. Brief pulses (1 ms) of millimolar concentrations of glutamate evoked membrane currents consisting of two kinetically distinct components in almost every membrane patch at −60 mV (Fig. 2*A*). The fast component was blocked by 10 μM CNQX in the external solution, and the slow component was abolished by 50 μM D-AP5. The effects of both antagonists were almost entirely reversible. Half-maximal inhibitory concentrations were 131 nM for CNQX ($n = 4$) and 1·40 μM for D-AP5 ($n = 10$), and Hill coefficients were close to 1 for both antagonists (data not shown). This suggests that the dual-component glutamate-activated currents in basket cells were mediated by AMPA/kainate- and NMDA-type GluRs, as in pyramidal neurones of the hippocampus (Jonas & Spruston, 1994; Spruston *et al.* 1995). The relative contribution of the two types of GluR channels was highly variable from cell to cell as illustrated by a scatter plot (Fig. 2*B*). The mean peak current ratio of the NMDA component to the AMPA/kainate component obtained by linear regression was 0·22 (range, 0·07–21; $n = 23$; 1 ms pulses of 10 mM glutamate), comparable to the mean value determined for pyramidal neurones (Spruston *et al.* 1995; Table 1).

Agonist preference of AMPA/kainate-type GluR channels expressed in basket cells

The AMPA/kainate receptor-mediated component of glutamate-activated currents in basket cell patches was studied in isolation in the absence of glycine and in the presence of 50 μM D-AP5 to block NMDARs. AMPARs and kainate receptors can be distinguished on the basis of agonist preference and desensitization properties (Wisden & Seeburg, 1993; Patneau, Vyklicky & Mayer, 1993; Partin, Patneau, Winters, Mayer & Buonanno, 1993; Lerma, Paternain, Naranjo & Mellström, 1993). To address the question of which type of GluR channel mediated this component, glutamate, AMPA and kainate were applied to hippocampal basket cell patches. Currents activated by 100 ms pulses of 1 mM glutamate at a membrane potential of −60 mV rose to a peak within 200–600 μs (20–80% rise time) and desensitized very rapidly, within a few milliseconds (Fig. 3*A*). Currents activated by 100 ms pulses of 1 mM AMPA showed a similar time course. For both agonists, desensitization was almost complete at the end of the 100 ms pulse, the amplitude of the non-desensitizing component being less than 1% of the peak current amplitude (Fig. 3*A*).

Application of kainate (1 mM, 100 ms) to basket cell patches evoked currents which, unlike the responses to

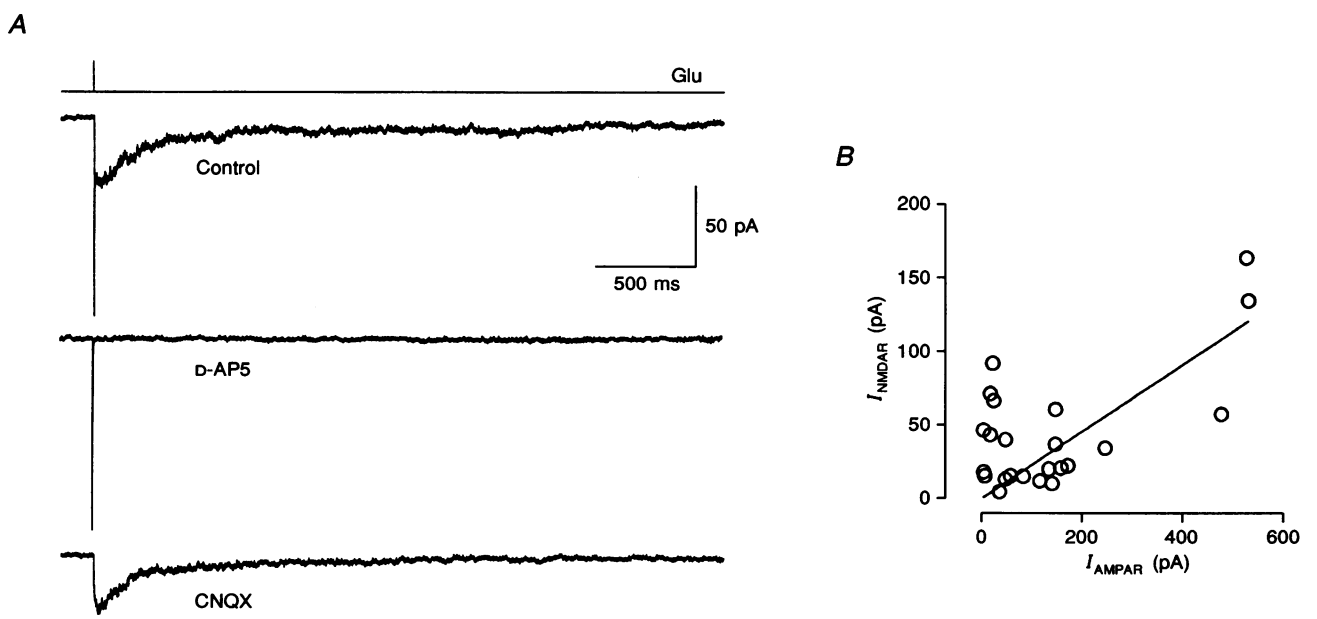

Figure 2. Dual-component glutamate-activated currents in basket cell patches

A, current traces obtained in Na^+-rich solution in the absence of external Mg^{2+} (Control) or with 50 μM D-AP5 or 10 μM CNQX from a basket cell patch. 1 ms pulses of 10 mM glutamate. *B*, scatter plot of NMDAR-mediated against AMPA/kainate receptor-mediated peak currents. NMDAR-mediated peak current amplitude was measured from the difference between recordings in the absence and in the presence of either Mg^{2+} or D-AP5. AMPA/kainate receptor-mediated peak current amplitude was measured in the presence of 1 mM external Mg^{2+} or 50 μM D-AP5. The straight line was obtained by linear regression through the origin. NMDAR-mediated and AMPA/kainate receptor-mediated peak currents were significantly correlated (correlation coefficient 0·63, $P < 0·001$). Na^+-rich external solution (10 μM glycine); membrane potential, −60 mV in all cases.

glutamate and AMPA, were only weakly desensitizing. With kainate, the amplitude of the non-desensitizing component was 60·2 ± 6·5% of that of the peak current ($n = 9$). The amplitude of the kainate-activated peak current was much smaller than that of the AMPA-activated peak current recorded in the same patches; on average it was only 17·5 ± 2·4% ($n = 4$) of the amplitude of the AMPA-activated peak current (Fig. 3*A*).

The concentration dependence of the peak conductance changes activated by the different agonists revealed that basket cell AMPA/kainate-type GluRs differed in their apparent affinity for glutamate, AMPA and kainate (Fig. 3*B*). The highest affinity was observed for AMPA; the half-maximal activating concentration (EC_{50}) was 423 μM (Hill coefficient, 1·15). The half-maximal activating concentrations for glutamate and kainate were both higher: 813 μM (Hill coefficient, 1·34) and 642 μM (Hill coefficient, 0·84), respectively. The EC_{50} values in basket cells were thus about twofold higher than in hippocampal pyramidal neurones (Jonas & Sakmann, 1992; Table 1). Pre-incubation with AMPA almost completely abolished kainate-activated currents (both agonists applied at roughly half-maximal activating concentrations of 300 and 500 μM, respectively), suggesting that AMPA and kainate activated the same GluR channel in basket cell patches ($n = 2$, data not shown; see Patneau & Mayer, 1991).

To address further the question as to whether kainate receptors contribute to the AMPA/kainate component of the glutamate-activated current in basket cell patches, the effect of cyclothiazide, a blocker of desensitization with high specificity for AMPA-preferring over kainate-preferring GluR channels (Partin *et al.* 1993), was investigated. Micromolar concentrations of cyclothiazide reversibly inhibited desensitization of glutamate-activated currents in basket cell patches (Fig. 4*A*). The half-maximal inhibition of desensitization was observed with a concentration of

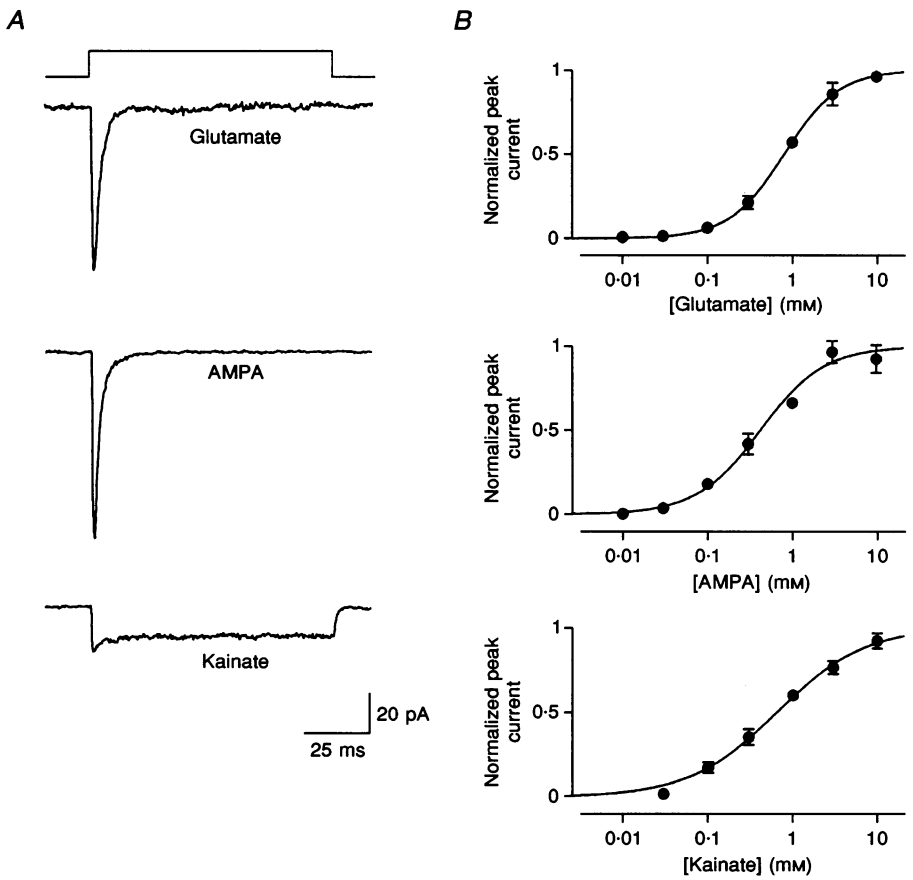

Figure 3. Activation of AMPA/kainate receptor channels in basket cell patches by different agonists

A, traces of current activated by 100 ms pulses (as indicated above the traces) of 1 mM glutamate, AMPA and kainate. Data were obtained from the same patch. *B*, concentration dependence of peak currents activated by glutamate ($n = 6$), AMPA ($n = 7$) and kainate ($n = 9$). Peak current amplitudes were normalized to the value obtained with 1 mM of the respective agonists and were fitted with the Hill equation (eqn (1)). Subsequently, the data points and the fitted curve were normalized to the extrapolated maximal value for high agonist concentrations estimated by least-squares fit. Half-maximal activating concentrations were 813, 423 and 642 μM and Hill coefficients were 1·34, 1·15 and 0·84, respectively. Na^+-rich external solution (glycine free, 50 μM D-AP5); membrane potential, −60 mV in all cases.

14·6 μM (Fig. 4*B*); high concentrations of cyclothiazide completely abolished desensitization (Fig. 4*A* and *B*).

In conclusion, the preferential activation by AMPA and the sensitivity of desensitization to cyclothiazide suggest that the 'AMPA/kainate' component in basket cell patches was mediated entirely by AMPARs (Partin *et al.* 1993; Patneau *et al.* 1993), presumably assembled from subunits of the GluR-A to -D (GluR1 to GluR4) family (Wisden & Seeburg, 1993). The contribution of kainate receptors appears to be negligible under the experimental conditions used.

Deactivation, desensitization and recovery of basket cell AMPARs from desensitization

Gating properties of AMPARs in hippocampal basket cells were studied using glutamate pulses of different durations (Fig. 5*A*). The *deactivation* time course of currents evoked by 1 ms pulses of 1 mM glutamate at −60 mV, reflecting the closure of channels after removal of the agonist, could be described by a single exponential with a mean time constant (τ) of 1·18 ± 0·11 ms (range, 0·67–1·37 ms; $n = 8$). In basket cells, deactivation of AMPARs was thus considerably faster than in principal neurones (Colquhoun *et al.* 1992; Table 1). The desensitization time course of currents activated by 100 ms pulses of 1 mM glutamate, reflecting the closure of channels in the maintained presence of the agonist, was characterized by a time constant of 3·72 ± 0·20 ms (range, 2·42–5·58 ms; $n = 22$) when fitted with a single exponential function. In many patches, however, the desensitization time course was better described using the sum of two exponentials (see Colquhoun *et al.* 1992; Spruston *et al.* 1995). The mean desensitization time constants obtained from the double-exponential fit were $\tau_1 = 2{\cdot}8 \pm 0{\cdot}2$ ms (79 ± 4·0% amplitude contribution) and $\tau_2 = 14{\cdot}2 \pm 2{\cdot}4$ ms (21 ± 4·0%, $n = 22$). The desensitization time constant of currents activated by 100 ms pulses of 1 mM AMPA in hippocampal basket cell patches was $\tau = 3{\cdot}31 \pm 0{\cdot}46$ ms ($n = 13$), almost the same as for glutamate. Desensitization kinetics of AMPARs in basket cells were thus about threefold faster than in hippocampal principal neurones under identical recording conditions (Colquhoun *et al.* 1992; Table 1).

Recovery of AMPARs from desensitization, which is potentially important for depression of synaptic currents, was studied using a double-pulse protocol, two 1 ms pulses of glutamate being separated by intervals of variable duration (Fig. 5*B*). These experiments revealed that the majority of AMPAR channels (on average 66%) were desensitized directly after the first 1 ms pulse of glutamate (Fig. 5*B* and *C*). Two exponential components were required to describe adequately the recovery of basket cell AMPARs from desensitization. The time constants of recovery were 33·8 ms (40% contribution to depression) and 387 ms (26%). Recovery kinetics of AMPARs from brief-pulse desensitization in basket cells were thus similar to those in granule cells of dentate gyrus, but were considerably slower than in hippocampal pyramidal cells (Colquhoun *et al.* 1992). The desensitization time constant measured using perforated vesicles (see Methods) was 3·97 ± 0·32 ms (monoexponential fit, $n = 4$), similar to that obtained in outside-out patches. In conclusion, AMPARs in basket cells were characterized by rapid deactivation and desensitization kinetics, but exhibited relatively slow recovery from desensitization.

Rectification of the peak *I–V* of AMPAR-mediated current in Na^+-rich external solution

Recombinant AMPARs assembled from various subunit combinations differ strikingly in current rectification and divalent permeability (Hollmann *et al.* 1991; Burnashev *et al.* 1992; Wisden & Seeburg, 1993). To allow a comparison of

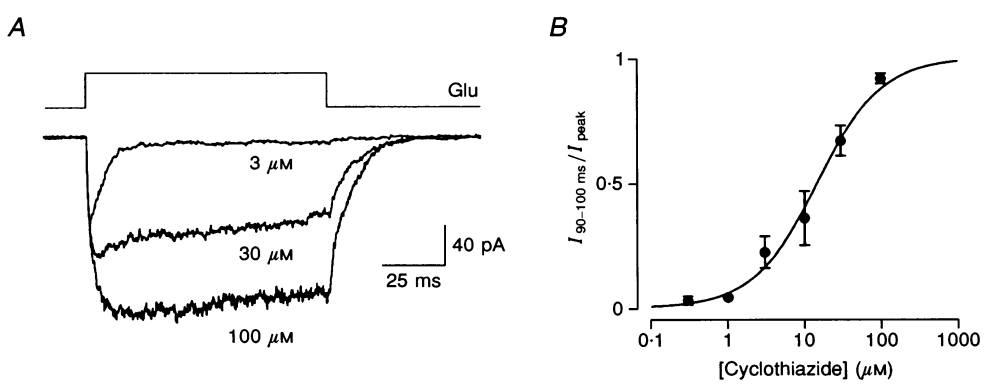

Figure 4. Inhibition of desensitization of basket cell AMPARs by cyclothiazide

A, traces with 3, 30 and 100 μM cyclothiazide in solutions in both barrels of the application pipette. 100 ms pulses of 1 mM glutamate. *B*, concentration dependence of cyclothiazide effects on desensitization. Ratio of mean current between 90 and 100 ms after beginning of the glutamate pulse and peak current was plotted against cyclothiazide concentration. Half-maximal effective concentration and Hill coefficient as obtained by least-squares fit with eqn (1) were 14·6 μM and 1·03, respectively. Data from 6 patches. Na^+-rich external solution (glycine free, 50 μM D-AP5); membrane potential, −60 mV in all cases.

native basket cell AMPARs with recombinant AMPARs, we studied current rectification. I–V relations for the glutamate-activated peak current in Na^+-rich external solution showed a mean reversal potential of $-4{\cdot}0 \pm 2{\cdot}6$ mV ($n = 14$), indicating an approximately equal permeability of AMPAR channels to Na^+ and K^+ ions (Fig. 6). In the majority of basket cell patches (13 of 14 patches) the I–V relation showed a doubly rectifying shape. The slope conductance was minimal between −20 and 0 mV and increased at very negative and positive potentials (Fig. 6*B*). To describe quantitatively the shape of the I–V relations, rectification indices were defined as the ratios of the slope conductance (g) at −80, −20 and 40 mV. On average, $g_{-80\ mV}/g_{-20\ mV}$ was $2{\cdot}54 \pm 0{\cdot}56$ (range, 1·26–8·39; $n = 12$), $g_{+40\ mV}/g_{-20\ mV}$ was $1{\cdot}43 \pm 0{\cdot}15$ (range, 0·86–2·78) and $g_{+40\ mV}/g_{-80\ mV}$ was $0{\cdot}74 \pm 0{\cdot}12$ (range, 0·11–1·62). These values indicate that the shape of the peak I–V relation in basket cell patches was clearly distinct from that in hippocampal principal neurones, which express AMPARs characterized by almost linear I–V relations (Colquhoun *et al.* 1992). The double rectification of the peak I–V of AMPARs in basket cell patches was, however, much less pronounced than that of the steady-state I–V of recombinant AMPARs lacking the edited form of GluR-B (Hollmann *et al.* 1991; Burnashev *et al.* 1992). The shape of the peak I–V in perforated vesicles was similar to that in outside-out patches, suggesting that washout of cytoplasmic factors e.g. proteins is unlikely to be responsible for the relatively weak rectification in our experiments.

Single-channel conductance of basket cell AMPARs

Recently it has been shown that the single-channel conductance of AMPARs differs between neuronal cell types (Hestrin, 1993; Livsey, Costa & Vicini, 1993; Jonas *et al.* 1993; Silver, Colquhoun, Cull-Candy & Edmonds, 1994; Spruston *et al.* 1995). In basket cell patches, transitions of single AMPARs between open and closed states were occasionally observed in individual traces

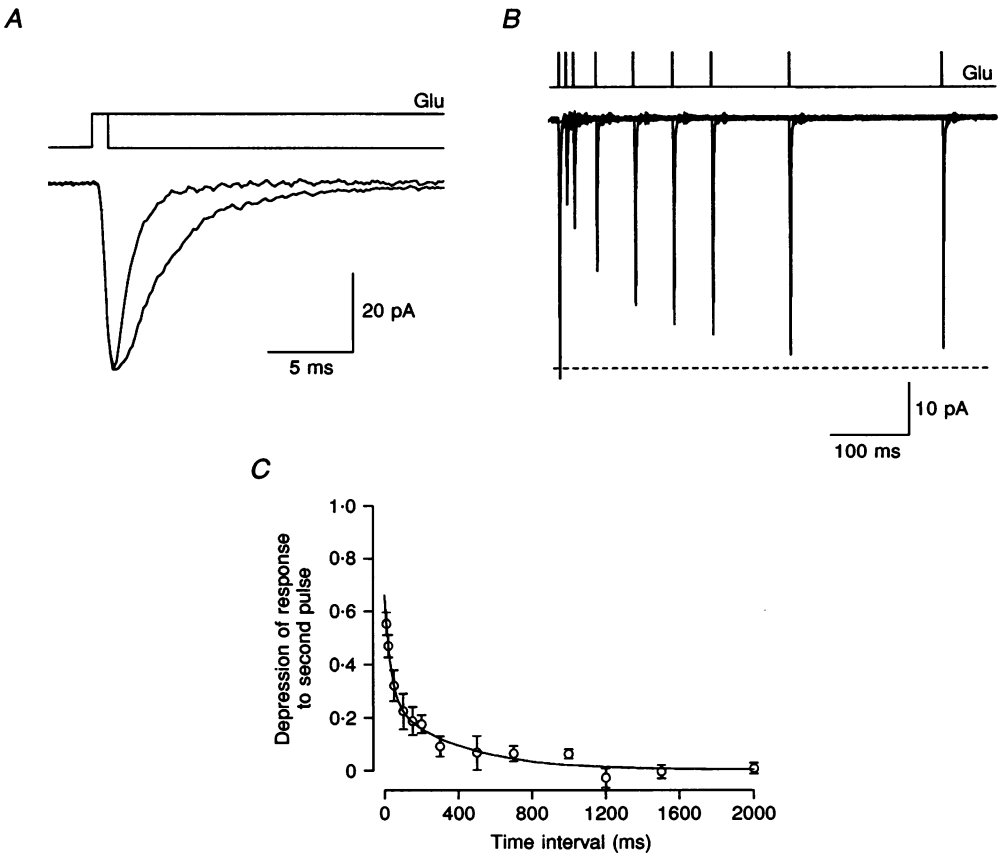

Figure 5. Time course of deactivation, desensitization and recovery from brief pulse desensitization of AMPAR channels in basket cell patches

A, superimposed current traces activated by 1 and 100 ms pulses of 1 mM glutamate. Deactivation time constant, 1·1 ms; desensitization time constant, 3·3 ms. *B*, responses to pairs of 1 ms pulses separated by increasing time intervals. Dashed horizontal line indicates the mean peak current amplitude during the first glutamate pulse. *C*, time course of recovery from brief-pulse desensitization. Data points were fitted by the sum of two exponential functions; $\tau_1 = 33{\cdot}8$ ms (40% contribution to depression) and $\tau_2 = 387$ ms (26%). Data pooled from 5 patches. Na^+-rich external solution (glycine free, 50 μM D-AP5); membrane potential, −60 mV in all cases.

Table 1. Comparison of functional properties of GluRs in hippocampal basket cells and principal neurones

	Basket cells	Principal neurones
I_{NMDAR}/I_{AMPAR}	0·22	0·21
AMPAR		
EC_{50} (AMPA) (μM)	423	183–189*
EC_{50} (glutamate) (μM)	813	342–424*
EC_{50} (kainate) (μM)	642	344–474*
IC_{50} (CNQX) (nM)	131	106–183†
Deactivation τ (ms)	1·18 ± 0·11	2·32–2·98†
Desensitization τ (ms)	3·72 ± 0·20	9·29–11·26†
Recovery τ_1 (ms)	33·8 (40%)	33 (41%, DG), 48 (60%, CA3), 58 (53%, CA1)†
Recovery τ_2 (ms)	387 (26%)	450 (33%, DG)†
γ (pS)	22·6 ± 1·6	8·6–10·2‡§
V_{rev} (mV) (Ca^{2+}/M^+)	13·4 ± 1·9 (Ca^{2+}/K^+)	−54·6 to −44·8†§ (Ca^{2+}/Cs^+, K^+)
NMDAR		
Activation τ (ms)	12·4 ± 2·2	4·8–8·8§
Deactivation τ_1 (ms)	266 ± 23 (76%)	175–288 (72–85%)§
Deactivation τ_2 (ms)	2620 ± 383 (24%)	1188–2918 (15–28%)§
Desensitization τ (ms)	470 ± 57	457–601§
γ (pS)	50·2 ± 1·8	44–46§
V_{rev} (mV) (Ca^{2+}/M^+)	31·8 ± 1·0 (Ca^{2+}/K^+)	31·4–31·6§ (Ca^{2+}/Cs^+)

Data for basket cells (first column) from this paper; data for principal neurones (dentate gyrus granule cells, CA3 and CA1 pyramidal cells; second column) from: * Jonas & Sakmann, 1992, † Colquhoun *et al.* 1992, ‡ Jonas *et al.* 1993, § Spruston *et al.* 1995. Percentages given in parentheses denote amplitude contribution of each exponential component. Recovery from desensitization (1 ms pulses) is given separately for dentate gyrus granule cells, CA3 and CA1 pyramidal cells, because in granule cells two exponentials were needed to describe recovery, whereas in pyramidal cells a single exponential was sufficient. Reversal potentials (V_{rev}) were measured with 100 mM $[Ca^{2+}]_o$; intracellular solutions were either K^+ or Cs^+ rich.

recorded in Na^+-rich external solution; selected records at −80 mV are shown in Fig. 7*A*. Single channel events were heterogeneous in current amplitude (between 15 and 50 pS) and were difficult to measure due to the rapid desensitization time course. The mean single-channel conductance was therefore estimated using non-stationary fluctuation analysis of AMPAR-mediated currents (Jonas *et al.* 1993; Spruston *et al.* 1995). Individual traces of current activated by 100 ms pulses of 3 mM glutamate at −80 mV showed fluctuation between trials (Fig. 7*B*). In Fig. 7*C*, the variance was plotted against the mean current. The single-channel conductance was estimated by fitting the data points using eqn (2), yielding a mean single-channel chord conductance γ of 22·6 ± 1·6 pS (range, 19·9–26·5 pS; $n = 5$), assuming a current reversal potential of 0 mV. The single-channel conductance was thus about twofold larger than that of AMPARs in hippocampal pyramidal neurones (Jonas *et al.* 1993; Spruston *et al.* 1995; Table 1). The mean value of the open probability of basket cell AMPARs at the peak was 0·54 ± 0·04 ($n = 5$) with 3 mM glutamate.

High Ca^{2+} permeability of basket cell AMPARs

The Ca^{2+} permeability of basket cell AMPAR channels was studied with different concentrations of Ca^{2+} in the external solution. When external monovalent cations were entirely replaced by Ca^{2+}, the reversal potential of the glutamate-activated peak current shifted to positive values, indicating a high Ca^{2+} permeability (Fig. 8*A* and *B*). On average, the measured value of the reversal potential with an external solution containing 100 mM Ca^{2+} was 13·4 ± 1·9 mV ($n = 17$; not corrected for liquid junction potentials), with no significant differences between glutamate ($n = 10$) and AMPA ($n = 7$) as the agonist ($P > 0·2$, *t* test). Reversal potentials with Ca^{2+}-rich external solution showed some variability between different cells (range, −2·7 to 24·2 mV), but in all cases the reversal potential was much more positive than in hippocampal granule cells (−43·8 ± 0·7 mV, $n = 4$; Fig. 8*B*) and pyramidal neurones (Colquhoun *et al.* 1992; Spruston *et al.* 1995; Table 1). Ca^{2+} permeability of AMPARs in basket cells from older rats (postnatal day 22) was similar ($n = 2$),

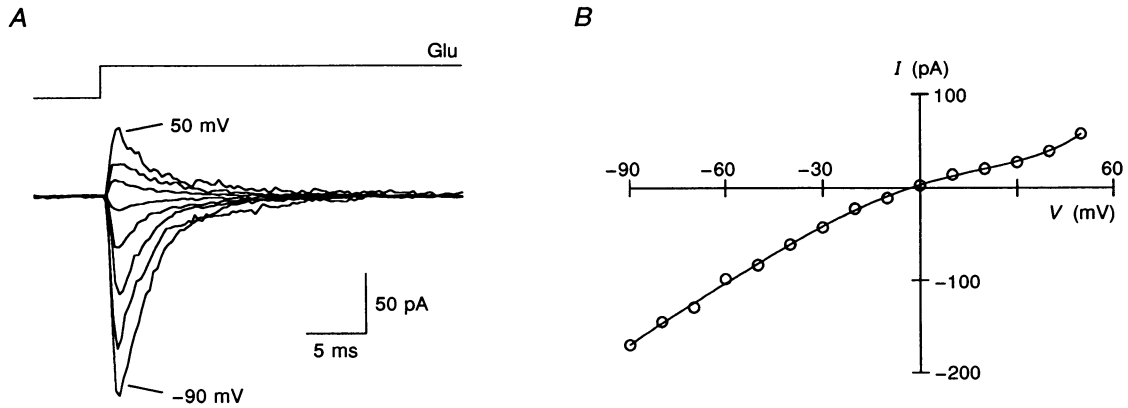

Figure 6. Rectification of AMPAR-mediated peak currents in Na^+-rich extracellular solution

A, membrane current traces evoked by long pulses of 1 mM glutamate. Membrane potential was varied between −90 and 50 mV in 20 mV steps. *B*, current–voltage (*I–V*) relation of glutamate-activated peak currents. Note the slight double rectification; $g_{-80\ mV}/g_{-20\ mV} = 1{\cdot}37$, $g_{+40\ mV}/g_{-20\ mV} = 0{\cdot}86$, and $g_{+40\ mV}/g_{-80\ mV} = 0{\cdot}63$ in this experiment. Na^+-rich external solution (glycine free, 50 μM D-AP5).

indicating the absence of developmental changes within this period.

To obtain a quantitative estimate of the relative Ca^{2+} permeability of basket cell AMPARs, the dependence of the reversal potential on the concentration of external Ca^{2+} was investigated (Fig. 8*C* and *D*). NMG^+ was used as a substitute for monovalent cations in the external solution, since AMPARs are not measurably permeable to NMG^+ (Iino *et al.* 1990; Jonas & Sakmann, 1992). When the $[Ca^{2+}]_o$ was increased from 1·8 to 100 mM, the reversal potential of the peak *I–V* shifted to positive values (Fig. 8*C*). A plot of the reversal potential (corrected for liquid junction potentials) against the activity of Ca^{2+} in the external solution summarizes the results from twenty-four membrane patches (Fig. 8*D*). The data points can be satisfactorily fitted using eqn (3), yielding an apparent relative Ca^{2+} permeability (P_{Ca}/P_K) of 1·79, which is severalfold higher than that in hippocampal principal neurones (Jonas & Sakmann, 1992; Colquhoun *et al.* 1992; Table 1).

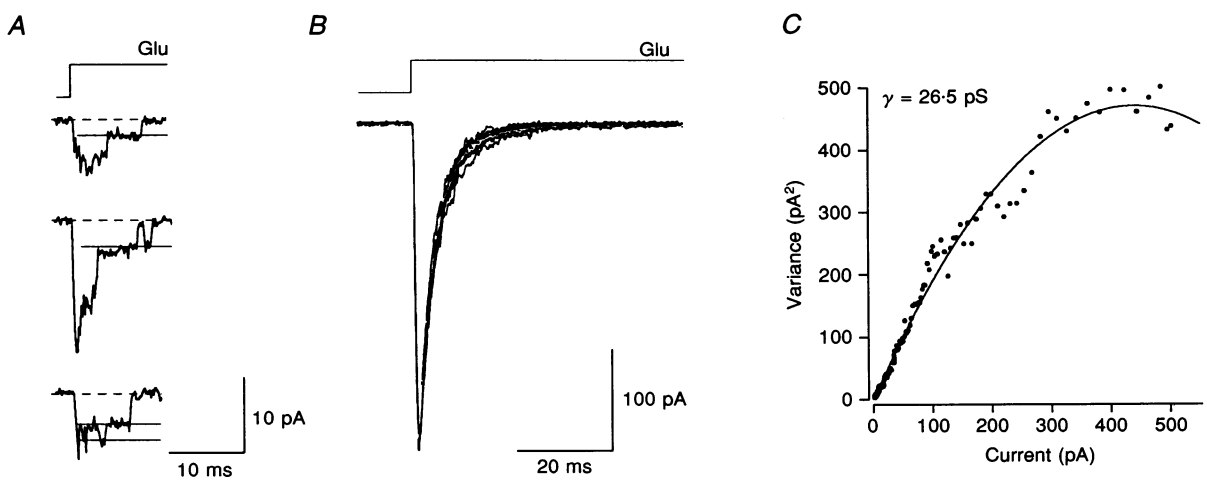

Figure 7. Single-channel conductance of basket cell AMPARs in Na^+-rich extracellular solution determined by non-stationary fluctuation analysis

A, selected single-channel currents. Recording bandwidth, 3 kHz (−3 dB). Dashed horizontal lines indicate baseline current when all channels are closed, and continuous lines denote open states. *B*, ten successive records obtained from a different outside-out patch are superimposed, together with their mean (white line). *C*, variance plotted against mean current for the same patch as shown in *B*. Data were obtained from 10 ensembles consisting of 10 records each. Data points were fitted using eqn (2), yielding a mean single-channel conductance of 26·5 pS and a maximal open probability of 0·57. Long pulses of 3 mM glutamate; Na^+-rich external solution (glycine free, 50 μM D-AP5); membrane potential, −80 mV in all cases.

Slow activation, deactivation and desensitization kinetics of basket cell NMDARs

The high Ca^{2+} permeability of AMPARs raises the question of how large the Ca^{2+} inflow via AMPARs is as compared with that via NMDARs. To address this issue, gating kinetics, current rectification properties and Ca^{2+} permeability of basket cell NMDARs were characterized in the presence of 10 μM glycine and 10 μM CNQX to block AMPARs.

In contrast to the rapid kinetics of AMPARs in basket cells, the rise, deactivation and desensitization time course of the pharmacologically isolated NMDAR-mediated component studied with glutamate pulses of different duration was very slow (Fig. 9). At −60 mV and in the absence of external Mg^{2+}, the 20–80% rise time was 12·4 ± 2·2 ms ($n = 5$; 1 ms, 1 mM glutamate pulse). A fit of the rising phase with an exponential function gave a mean rise time constant of 12·6 ± 1·6 ms, slightly higher than that of NMDARs in pyramidal neurones (Spruston *et al.* 1995; Table 1). The time course of deactivation of basket cell NMDARs was bi-exponential (Fig. 9*A*), with mean time constants $\tau_1 = 266 \pm 23$ ms ($n = 9$; 76% amplitude contribution) and $\tau_2 = 2620 \pm 383$ (24%). In the continuous presence of glutamate, NMDAR channels desensitized with a time constant of 470 ± 57 ms ($n = 5$; 7 s, 1 mM glutamate pulse). Desensitization of NMDARs was incomplete; the mean amplitude of the non-desensitizing component was 33% of that of the peak current (Fig. 9*B*). Deactivation and desensitization kinetics of NMDARs expressed in hippocampal basket cells were thus similar to those of NMDARs in principal neurones (Spruston *et al.* 1995; Table 1).

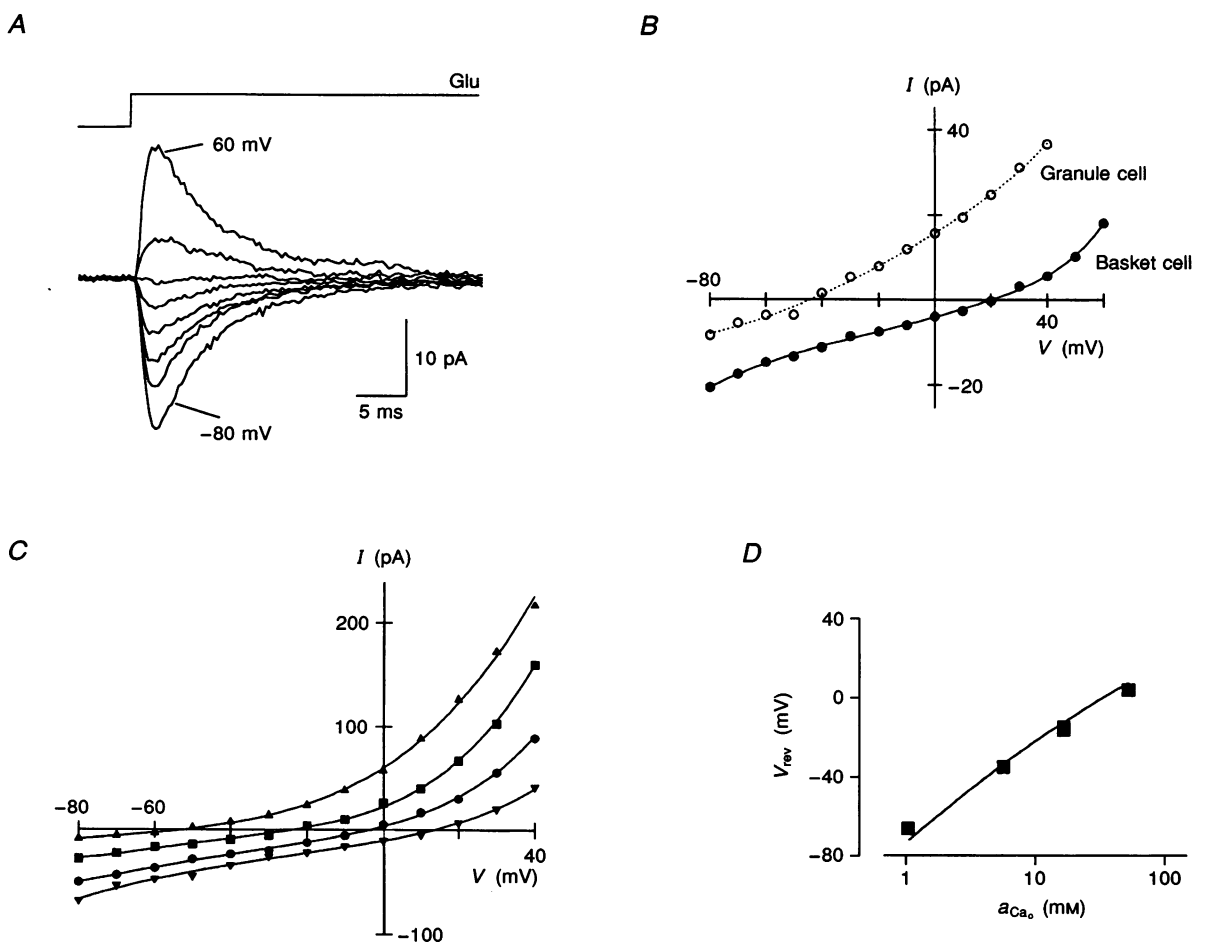

Figure 8. High Ca^{2+} permeability of AMPAR channels in basket cells of dentate gyrus

A, records from a basket cell patch in 100 mM $[Ca^{2+}]_o$ external solution (glycine free, 50 μM D-AP5). Current was activated by long pulses of 1 mM glutamate. Membrane potential was varied between −80 and 60 mV in 20 mV steps. *B*, *I–V* relations of peak currents in a basket cell patch (●, corresponding traces illustrated in *A*) and in a granule cell patch (○). Measured reversal potentials were 20·8 and −44·1 mV, respectively. *C*, *I–V* relations of peak currents in external solutions with 1·8 (▲), 10 (■), 30 (●), and 100 mM (▼) $[Ca^{2+}]_o$. Measured reversal potentials were −53·1, −24·3, −3·0 and 13·1 mV, respectively. All data from the same patch, different from that shown in *A* and *B*. *D*, reversal potential (V_{rev}, corrected for liquid junction potentials as described in Methods) plotted against extracellular Ca^{2+} activity (a_{Ca_o}). Data points were fitted using eqn (3), yielding a P_{Ca}/P_K of 1·79. Data pooled from 24 patches.

Rectification and Mg^{2+} block of basket cell NMDARs

I–V relations of the NMDAR-mediated peak current in Na^+-rich external solution showed a reversal potential of $1{\cdot}5 \pm 0{\cdot}6$ mV ($n = 3$), indicating an almost equal permeability to Na^+ and K^+ ions (Fig. 10*A* and *B*). The rectification properties of NMDAR-mediated currents were strongly dependent on the concentration of external Mg^{2+}. In the absence of Mg^{2+}, the peak *I–V* of the NMDAR-mediated glutamate-activated current was only slightly outwardly rectifying (Fig. 10*C*). In the presence of external Mg^{2+}, the *I–V* relation showed a region of negative slope conductance (Fig. 10*C*) due to the voltage-dependent block of NMDARs by these ions (Ascher & Nowak, 1988; Spruston *et al.* 1995). 1 mM Mg^{2+} almost completely abolished NMDAR-mediated currents at membrane potentials below −80 mV, whereas currents at positive potentials were not affected or even slightly enhanced (Fig. 10*C*). The maximal inward current in the presence of 1 mM Mg^{2+} was observed at −20 mV, similar to NMDAR-mediated currents in pyramidal cells (Spruston *et al.* 1995).

To describe quantitatively the shape of the *I–V* relation in the presence of external Mg^{2+}, data points were fitted using Woodhull's theory of voltage-dependent block, assuming a single binding site for the blocking ion located within the pore (Woodhull, 1973; eqn (4)). It was not intended to imply a particular mechanism of the block, but rather to provide an empirical description of the *I–V* of the NMDAR-mediated current necessary for the simulations (see Discussion). This analysis revealed apparent values for δ and K_0 of $0{\cdot}91 \pm 0{\cdot}08$ and $2{\cdot}91 \pm 1{\cdot}49$ mM, respectively, for 0·1 mM Mg^{2+} ($n = 3$) and $1{\cdot}13 \pm 0{\cdot}16$ and $7{\cdot}35 \pm 2{\cdot}87$ mM, respectively, for 1 mM Mg^{2+} ($n = 3$). The value of δ larger than 1 in the presence of 1 mM external Mg^{2+} indicates that the mechanism of block of NMDAR-mediated currents by Mg^{2+} is more complicated than implied by Woodhull's theory.

Single-channel conductance of NMDARs in basket cells

The single-channel conductance of basket cell NMDARs was measured in the absence of external Mg^{2+} in patches containing only a small number of channels (Fig. 11*A*). A single-channel *I–V* relation for the main open state is shown in Fig. 11*B* (data averaged, $n = 5$). The *I–V* relation

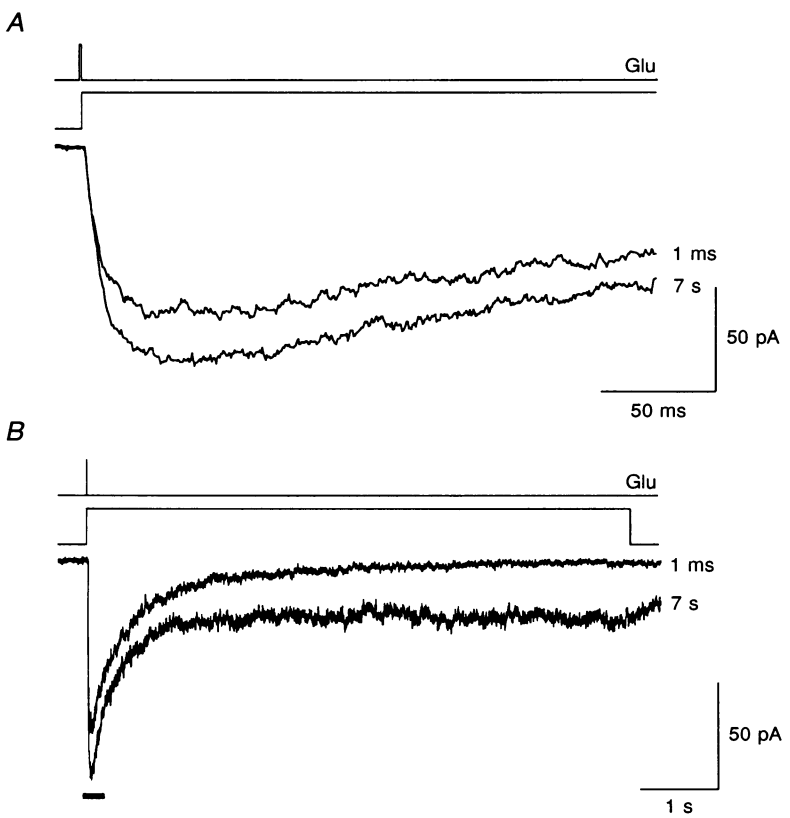

Figure 9. Rise time, deactivation and desensitization time course of basket cell NMDAR channels

A, rise time course. *B*, deactivation and desensitization kinetics. Same traces at different time scale; horizontal bar in *B* (below the traces) indicates the time range shown in *A*. Superimposed current traces activated by 1 ms and 7 s pulses of 1 mM glutamate. 20–80% rise time was 10·7 and 8·9 ms for current activated by 1 ms and 7 s pulses, respectively. The deactivation time constants were 363 (87%) and 1864 ms (13%), and the desensitization time constant was 371 ms in this patch. Na^+-rich external solution (10 μM glycine, 10 μM CNQX). Membrane potential, −60 mV.

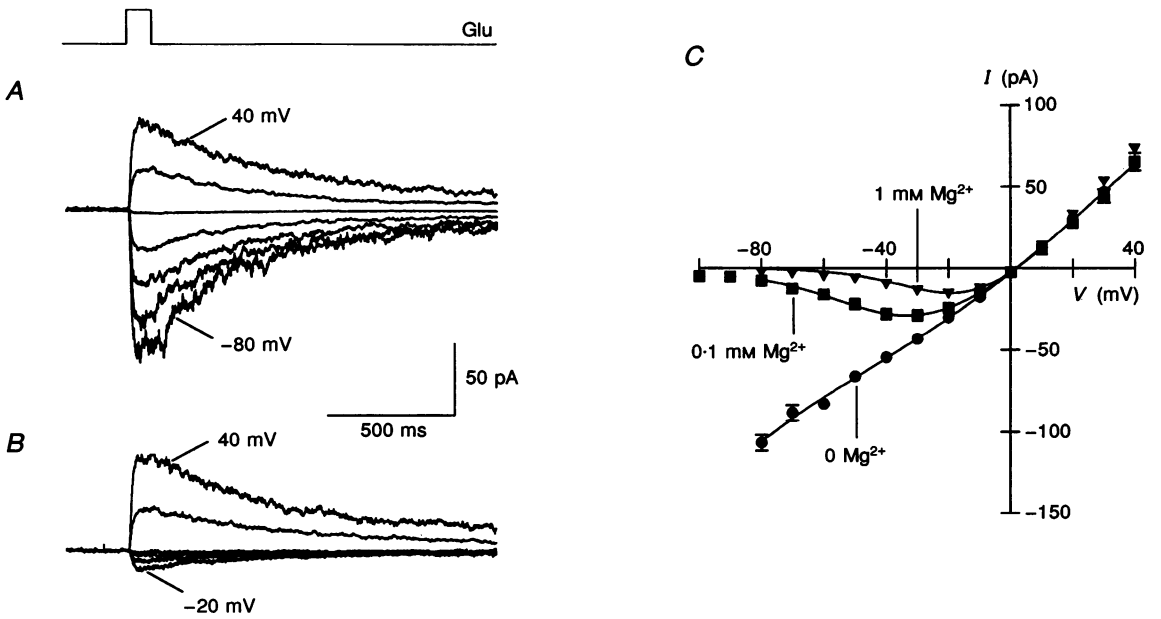

Figure 10. Rectification and Mg^{2+} block of NMDAR-mediated peak currents

A and *B*, traces obtained from a basket cell patch in Na^+-rich extracellular solution containing 0 (*A*) or 1 mM Mg^{2+} (*B*). Current was activated by 100 ms pulses of 100 μM glutamate. Membrane potential was varied between −80 and 40 mV in 20 mV steps. *C*, *I–V* relations of peak currents in external solutions containing 0 (●), 0·1 (■) and 1 mM Mg^{2+} (▼). Same patch as *A* and *B*. Data points were fitted using eqn (4), yielding $K_0 = 6{\cdot}02$ mM and $\delta = 1{\cdot}13$ for ▼ and $K_0 = 1{\cdot}49$ mM and $\delta = 0{\cdot}85$ for ■. Na^+-rich external solution (10 μM glycine, 10 μM CNQX) in all cases.

was approximately linear with a reversal potential close to 0 mV. The mean elementary conductance of basket cell NMDAR channels was $50{\cdot}2 \pm 1{\cdot}8$ pS ($n = 5$; Fig. 11), comparable to the value reported for NMDARs in pyramidal neurones (Spruston *et al.* 1995; Table 1). Subconductance states were occasionally observed but were not analysed in detail.

High Ca^{2+} permeability of basket cell NMDARs

The relative Ca^{2+} permeability of basket cell NMDARs was measured with an experimental protocol similar to that used for AMPARs. When monovalent cations in the external solution were entirely replaced by 100 mM Ca^{2+}, the reversal potential of the NMDAR-mediated component shifted to positive values (Fig. 12*A* and *B*). In basket cell

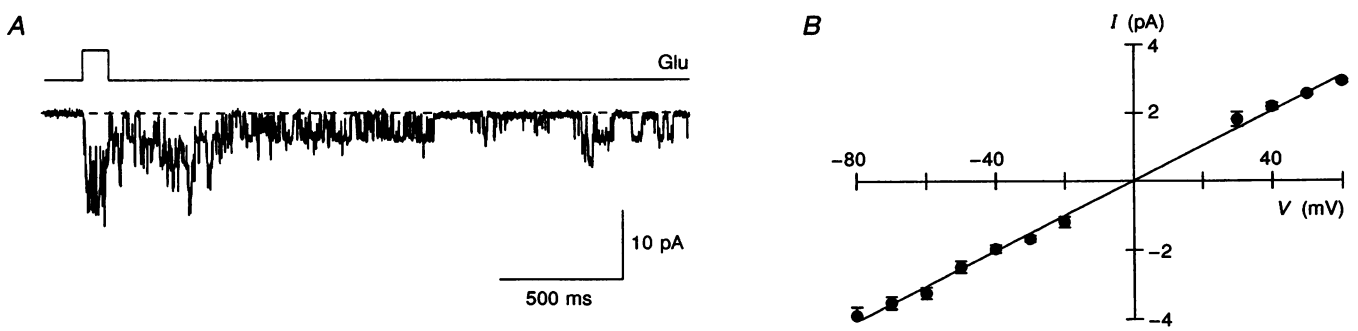

Figure 11. Single-channel conductance of basket cell NMDAR channels

A, individual trace obtained from a basket cell patch in Na^+-rich extracellular solution in the absence of Mg^{2+}. Membrane potential was −80 mV. Dashed horizontal line indicates current when all channels are closed. *B*, *I–V* relation for the main open state in the absence of Mg^{2+}; data pooled from five patches. Linear regression yielded a single-channel conductance of 50·2 pS and a reversal potential of 0 mV. Currents were activated by 100 ms pulses of 100 μM glutamate. Na^+-rich external solution (10 μM glycine, 10 μM CNQX) in all cases.

patches, the measured reversal potential of NMDAR-mediated peak current in these conditions was 31·8 ± 1·0 mV ($n = 6$; range, 27·5–34·9 mV; not corrected for liquid junction potentials), close to that in pyramidal cells (31·4–31·6 mV; Spruston *et al.* 1995) and granule cells (29·0 ± 1·9 mV, $n = 3$, Fig. 12*B*).

To obtain an estimate of the relative Ca^{2+} permeability of basket cell NMDARs, the dependence of the reversal potential on the external Ca^{2+} activity was investigated (Fig. 12*C* and *D*). Fitting of data points with eqn (3) yielded an apparent P_{Ca}/P_K of basket cell NMDARs of 6·68, similar to the high Ca^{2+} permeability reported in hippocampal principal neurones and in other types of cells (Ascher & Nowak, 1988; Spruston *et al.* 1995).

DISCUSSION

In this paper the functional properties of AMPAR and NMDAR channels in the basket cell of the hippocampal dentate gyrus are described. This GABAergic interneurone is readily identified in hippocampal slices on the basis of location and shape of the soma, architecture of the proximal dendrites and action potential pattern following sustained current injection. Using fast application of glutamate, we found that AMPARs and NMDARs were present in membrane patches isolated from basket cell somata. The functional properties of AMPARs in basket cells were strikingly different from those in principal neurones, whereas for NMDARs no major differences were found between the two classes of cells (Colquhoun *et al.* 1992; Spruston *et al.* 1995; Table 1).

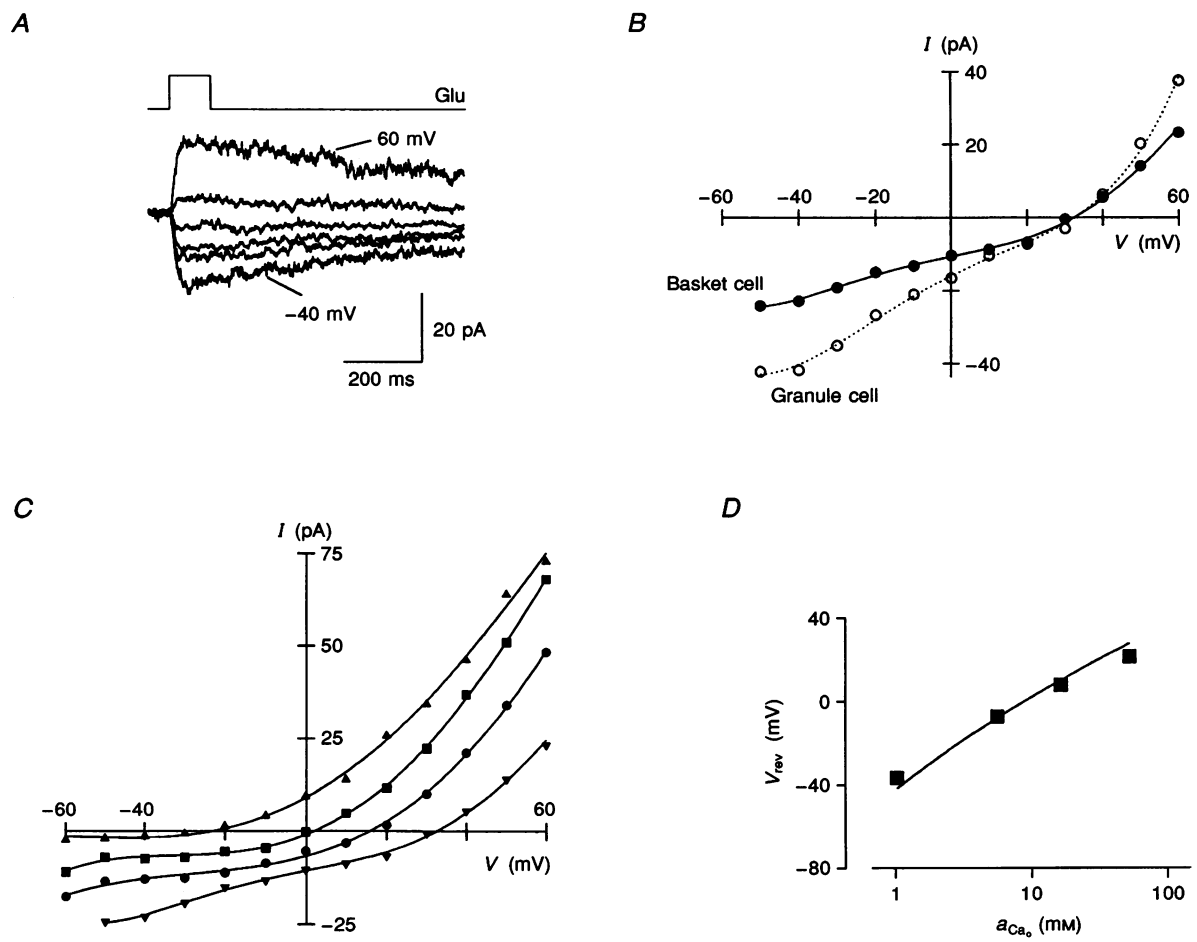

Figure 12. Ca^{2+} permeability of basket cell NMDAR channels

A, traces recorded from a basket cell patch in 100 mM $[Ca^{2+}]_o$ solution (10 μM glycine, 10 μM CNQX). Current was activated by 100 ms pulses of 100 μM glutamate. Membrane potential was varied between −40 and 60 mV in 20 mV steps. *B*, *I–V* relations of peak currents in a basket cell patch (●, corresponding traces illustrated in *A*) and in a granule cell patch (○). Measured reversal potentials were 31·1 and 32·4 mV, respectively. *C*, *I–V* relations of peak currents with external solutions containing 1·8 (▲), 10 (■), 30 (●), and 100 mM (▼) Ca^{2+}. ●, same patch as shown in *A* and *B*. Measured reversal potentials were −23·9, 1·9, 15·7 and 31·1 mV, respectively. *D*, V_{rev} (corrected for liquid junction potentials) plotted against extracellular Ca^{2+} activity (a_{Ca_o}). Fit using eqn (3) yields a P_{Ca}/P_K of 6·68. Data pooled from 16 patches.

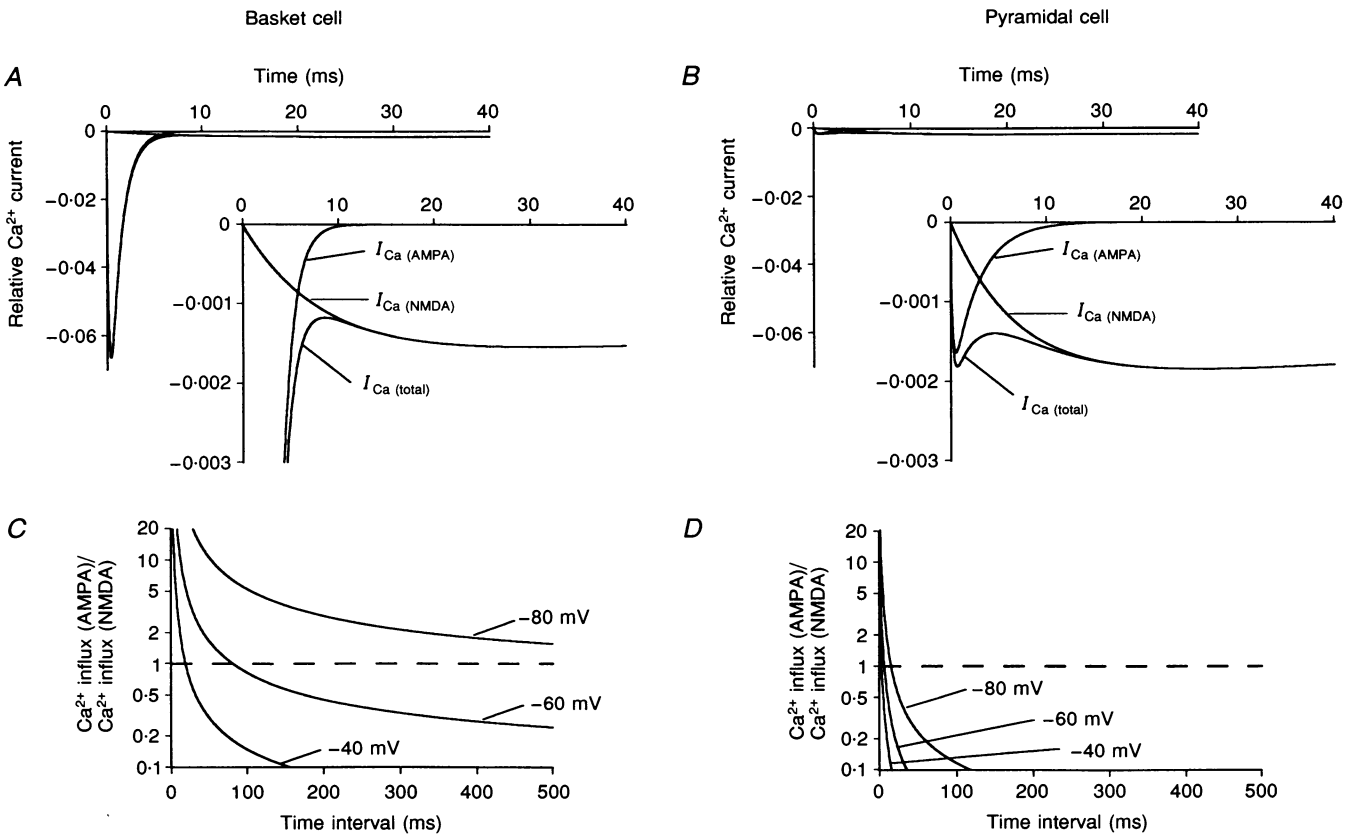

Figure 13. Simulation of Ca^{2+} influx through AMPARs and NMDARs in a basket cell and pyramidal cell during a dual-component conductance change

A and *B*, relative Ca^{2+} current in physiological extracellular solution (1 mM Mg^{2+}, 1·8 mM Ca^{2+}). Simulation for basket cell GluRs (*A*) and pyramidal cell GluRs (*B*). Ca^{2+} current amplitude is given relative to the peak amplitude of the total glutamate-evoked inward current carried by monovalent cations at −60 mV. Ca^{2+} current during dual-component conductance change, the AMPAR component and the NMDAR component are shown. The insets were expanded vertically to illustrate the relative Ca^{2+} current through NMDARs. Membrane potential, −60 mV. *C* and *D*, ratio of the amount of Ca^{2+} flowing through AMPARs to that entering through NMDARs during a glutamate-activated current. The amount of Ca^{2+} influx through each of the two channel types was obtained by integration of the respective Ca^{2+} current within a given time interval (beginning at 0 ms). The ratio of Ca^{2+} influx (AMPAR)/Ca^{2+} influx (NMDAR) is plotted against the duration of the integration interval. Dashed horizontal line indicates a ratio of 1. Simulation for basket cell GluRs (*C*) and pyramidal cell GluRs (*D*). Simulated curves are shown for

	Basket cell GluRs (this paper)	Pyramidal cell GluRs (Spruston *et al.* 1995)
I_{NMDAR}/I_{AMPAR}	0·22 (see Fig. 2)	0·21
$\tau_{AMPAR\ rise}$	0·2 ms	0·2 ms
$\tau_{AMPAR\ decay}$	1·2 ms	2·78 ms
$\tau_{NMDAR\ rise}$	8 ms	6·85 ms
$\tau_{NMDAR\ decay\ 1}$	266 ms (78%)	223 ms (79%)
$\tau_{NMDAR\ decay\ 2}$	2620 ms (22%)	2054 ms (21%)
$I_{AMPA}(V)$	*	$16{\cdot}67V$
$I_{NMDA}(V)$†	$\delta = 1{\cdot}13$, $K_0 = 7{\cdot}35$ mM	$\delta = 0{\cdot}8$, $K_0 = 4{\cdot}1$ mM
$P_{Ca}/P_{K\ AMPAR}$	1·79	0·04
$P_{Ca}/P_{K\ NMDAR}$	6·68	2·95

* $0{\cdot}0743 + 15{\cdot}72V - 35{\cdot}64V^2 + 706{\cdot}4V^3 + 22840V^4 + 195400V^5$. I_{AMPA} given relative to value at −60 mV and V given in volts. † $I_{NMDA}(V)$ according to eqn (4) with $[Mg^{2+}]_o = 1$ mM. For both types of cells, P_f values were calculated from the P_{Ca}/P_K values using eqn (5).

Functional properties of AMPARs in basket cells

AMPARs expressed in hippocampal basket cells differ from those in hippocampal pyramidal and granule cells in several respects. They have rapid kinetics (deactivation $\tau \approx 1$ ms, desensitization $\tau \approx 3$–4 ms), a doubly rectifying shape of the peak I–V relation in Na^+-rich extracellular solution, high apparent single-channel conductance (~23 pS), and high permeability to Ca^{2+} ions ($P_{Ca}/P_K \approx 1{\cdot}8$). In contrast, AMPARs in dentate gyrus granule cells and CA3 and CA1 pyramidal neurones show slower kinetics (deactivation $\tau \approx 2{\cdot}5$ ms, desensitization $\tau \approx 9$–11 ms), a linear peak I–V in Na^+-rich extracellular solution, low apparent single-channel conductance (~10 pS), and low Ca^{2+} permeability ($P_{Ca}/P_K \approx 0{\cdot}05$; Colquhoun *et al.* 1992; Spruston *et al.* 1995; Table 1).

Rapid desensitization kinetics appear to be a functional signature of AMPARs in GABAergic interneurones throughout the CNS. To date, rapidly desensitizing AMPARs have been found in aspiny hilar interneurones of hippocampal slices ($\tau \approx 3{\cdot}3$ ms, fast component; Livsey *et al.* 1993) and in non-pyramidal interneurones of neocortical slices ($\tau \approx 3{\cdot}4$ ms, Hestrin, 1993; $\tau \approx 5{\cdot}1$ ms, Jonas *et al.* 1994). A large single-channel conductance has also been reported for both hippocampal hilar interneurones (Livsey *et al.* 1993) and neocortical interneurones (27 pS; Hestrin, 1993).

High Ca^{2+} permeability of AMPARs appears to be characteristic for the majority but not all types of interneurones. So far, Ca^{2+}-permeable AMPARs have been found in non-pyramidal neurones in neocortical slices; P_{Ca}/P_K was, however, lower than in basket cells reported here (0·63 *vs.* 1·79; Jonas *et al.* 1994). In addition, a subset of interneurones in the CA3 region of hippocampal slices shows an inwardly rectifying I–V relation of kainate-activated current (McBain & Dingledine, 1993), possibly indicative for the expression of Ca^{2+}-permeable AMPARs. Finally, a GABAergic subpopulation of cultured hippocampal neurones (type II cells) expresses Ca^{2+}-permeable AMPARs ($P_{Ca}/P_{Cs} = 2{\cdot}3$; Iino *et al.* 1990; Bochet *et al.* 1994). AMPARs in aspiny (presumably GABAergic) hilar interneurones, however, appear to be only weakly permeable to Ca^{2+} (Livsey *et al.* 1993). This suggests heterogeneity of interneurone AMPARs in the CNS with respect to Ca^{2+} permeability.

The molecular mechanisms underlying the distinct functional properties of basket cell AMPARs may be revealed by a comparison of native receptors and recombinant channels assembled from various subunit combinations. Subunit-specific differences in kinetics have been observed for recombinant AMPARs expressed in a mammalian cell line (Burnashev *et al.* 1992; Burnashev, 1993). The desensitization time course is fast for homomeric channels assembled from GluR-A or -D subunits, slow for GluR-B or -C homomers, and intermediate for heteromeric channels, e.g. GluR-A/B.

Rectification properties and Ca^{2+} permeability of recombinant AMPAR channels are determined by the GluR-B subunit in its edited form (for review see Wisden & Seeburg, 1993). Recombinant channels lacking the GluR-B subunit show doubly rectifying I–Vs and high Ca^{2+} permeability ($P_{Ca}/P_{Cs} \approx 1{\cdot}5$). Channels with higher GluR-B content show linear or outwardly rectifying I–Vs and low Ca^{2+} permeability ($P_{Ca}/P_{Cs} \approx 0{\cdot}05$). Depending on the relative abundance of GluR-B mRNA, AMPARs with various intermediate rectification and conductance properties are formed (Burnashev *et al.* 1992).

Preliminary single cell mRNA analysis using the polymerase chain reaction (Jonas *et al.* 1994) suggested that the relatively high abundance of GluR-D and the low abundance of GluR-B subunit mRNA were responsible for the rapid kinetics and the high Ca^{2+} permeability of basket cell AMPARs (H. Monyer, J. R. P. Geiger, T. Melcher & P. Jonas, unpublished observations). The relative abundance of GluR-B mRNA showed variability between different basket cells, providing an explanation for the variability in Ca^{2+} permeability of native AMPARs.

Ca^{2+} influx through GluRs in basket and pyramidal cells of hippocampus

To assess the possible functional importance of the higher Ca^{2+} permeability of AMPARs in basket cells than in pyramidal cells, we simulated the relative Ca^{2+} current (defined as the current carried by Ca^{2+}, when normalized with respect to the peak of the total current activated by glutamate). A dual-component conductance change produced by a brief glutamate pulse in physiological extracellular solution (1 mM Mg^{2+}, 1·8 mM Ca^{2+}) was simulated for a basket cell and a pyramidal cell. At −60 mV, close to the resting membrane potential, the peak of the relative Ca^{2+} current through AMPARs in the basket cell was 43-fold larger than that through NMDARs (Fig. 13*A*). In contrast, the peaks of the relative Ca^{2+} currents through AMPARs and NMDARs in the pyramidal neurone were similar in amplitude (Fig. 13*B*).

To compare the inflow of Ca^{2+} through AMPARs and NMDARs, the ratio of Ca^{2+} influx (AMPAR) to Ca^{2+} influx (NMDAR) was calculated for various integration intervals and membrane potentials. The influx ratio was severalfold higher in basket cells (Fig. 13*C*) than in pyramidal cells (Fig. 13*D*) in all conditions. For example, during the first 100 ms of the glutamate-activated Ca^{2+} current, the ratio was 0·83 at −60 mV in basket cells, whereas it was 0·03 in pyramidal cells. As the deactivation of AMPARs is much faster than that of NMDARs, the influx ratio decreases monotonically as the integration interval increases. This indicates a significant contribution of basket cell AMPARs to Ca^{2+} influx predominantly in the early phase of the glutamate-activated current. Also, since depolarization relieves the Mg^{2+} block of NMDARs, the relative contribution of AMPARs becomes smaller when the cell depolarizes.

The simulations thus imply that during activation by brief glutamate pulses, as may occur during synaptic transmission, the Ca^{2+} inflow through AMPARs in basket cells is comparable to that through NMDARs at resting or subthreshold membrane potentials and for short integration intervals, whereas NMDAR channels are the main source at more positive potentials. In pyramidal cells in almost all conditions, NMDAR channels are the main mediators of Ca^{2+} inflow through the postsynaptic membrane.

Excitatory synapses on basket cells are spontaneously active at high rates (Schwartzkroin & Mathers, 1978, for basket cells in the CA1 subfield). Because of the voltage dependence of the influx ratio, the relative contribution of AMPARs to Ca^{2+} entry in basket cells is expected to be larger during spontaneous miniature excitatory postsynaptic potentials than during evoked events that lead to stronger membrane depolarization or action potential initiation. Thus, if postsynaptic AMPAR channels are similar to those in the soma membrane, there would be a synaptically mediated Ca^{2+} influx into basket cells at rest.

The estimates of relative Ca^{2+} currents represent only first approximations. First, a wide variability in the relative Ca^{2+} entry through AMPARs as compared with NMDARs in different basket cells or different synapses is anticipated on the basis of the scatter of the relative contributions of both types of receptors to the glutamate-activated currents in patches (Fig. 2*B*). Second, combined $[Ca^{2+}]_i$ fluorescence and whole-cell current measurements revealed that the measured Ca^{2+} influx through recombinant GluRs in physiological conditions is smaller than that predicted using the P_{Ca}/P_M ratio and the GHK equation (Burnashev *et al.* 1995). Simulations using fractional Ca^{2+} currents measured for recombinant channels (GluR-A or GluR-D and NR1/NR2A or NR1/NR2C; Burnashev *et al.* 1995) resembling the putative subunit composition of basket cell GluRs yielded an influx ratio of 0·97 at −60 mV for an integration interval of 100 ms. This ratio is only slightly different from that predicted from the P_{Ca}/P_M values of basket cell GluRs (Fig. 13*C*; the ratio was 0·83 at −60 mV for the same integration interval).

Implications for excitatory synaptic transmission between principal neurones and interneurones

Provided that the functional properties of AMPARs and NMDARs in the postsynaptic membrane are similar to those in somatic membrane patches, the characteristic properties of GluR channels in basket cells might influence both synaptic efficacy and Ca^{2+} signalling.

The AMPAR-mediated excitatory postsynaptic current (EPSC) components in basket cells could exhibit a faster decay time course than those in principal neurones. Rapidly rising and decaying AMPAR-mediated EPSCs have been recorded in basket cells (20–80% rise time < 200 μs; decay $\tau \approx 1$ ms; J. R. P. Geiger & P. Jonas, unpublished observations) which may reflect both the rapid kinetics of AMPARs and the somatic location of excitatory synapses (Ribak & Seress, 1983). Comparatively fast decays of AMPAR-mediated EPSCs have also been reported for aspiny hilar interneurones (Livsey & Vicini, 1992).

Basket cell AMPARs are characterized by profound desensitization following brief glutamate pulses and a slow recovery from desensitization. Excitatory synaptic transmission between pyramidal and basket cells in the CA3 subfield of the hippocampus appears to be predominantly mediated by a single release site (Gulyás, Miles, Sík, Tóth, Tamamaki & Freund, 1993). The majority of AMPARs of a synapse between a principal neuron and a basket cell thus could have a refractory period (after activation by synaptically released glutamate) which is determined by the kinetics of recovery from desensitization. The function of rapid desensitization of AMPARs at basket cell synapses appears to be different from that in calyceal synapses on cochlear nucleus neurones, where rapid desensitization was proposed to minimize the effects of interaction between transmitter quanta released from neighbouring sites (Trussell, Zhang & Raman, 1993).

The present results also suggest a dual pathway for synaptically mediated Ca^{2+} entry into basket cells. The increase of $[Ca^{2+}]_i$ at the synapse mediated by the two types of GluR channels should differ in their temporal characteristics. AMPARs are likely to generate a rapid, transient increase in $[Ca^{2+}]_i$, whereas NMDARs mediate a longer lasting increase. Interestingly, subsets of basket cells (and other types of GABAergic interneurones) specifically express the Ca^{2+}-binding protein parvalbumin (Ribak, Nitsch & Seress, 1990). The AMPAR-mediated transient Ca^{2+} inflow may be buffered less efficiently than the NMDAR-mediated inflow, since parvalbumin (e.g. from skeletal muscle) acts as a $[Ca^{2+}]_i$ buffer with slow kinetics at physiological $[Mg^{2+}]_i$ (Hou, Johnson & Rall, 1991). The possibly different functional effects of synaptic Ca^{2+} entry through AMPARs and NMDARs, e.g. for the activation of $[Ca^{2+}]_i$-dependent ion channels or synaptic plasticity, remain to be elucidated.

Ascher, P. & Nowak, L. (1988). The role of divalent cations in the *N*-methyl-D-aspartate responses of mouse central neurones in culture. *Journal of Physiology* **399**, 247–266.

Bliss, T. V. P. & Collingridge, G. L. (1993). A synaptic model of memory: long-term potentiation in the hippocampus. *Nature* **361**, 31–39.

Bochet, P., Audinat, E., Lambolez, B., Crépel, F., Rossier, J., Iino, M., Tsuzuki, K. & Ozawa, S. (1994). Subunit composition at the single-cell level explains functional properties of a glutamate-gated channel. *Neuron* **12**, 383–388.

Burnashev, N. (1993). Recombinant ionotropic glutamate receptors: functional distinctions imparted by different subunits. *Cellular Physiology and Biochemistry* **3**, 318–331.

Burnashev, N., Monyer, H., Seeburg, P. H. & Sakmann, B. (1992). Divalent ion permeability of AMPA receptor channels is dominated by the edited form of a single subunit. *Neuron* **8**, 189–198.

Burnashev, N., Zhou, Z., Neher, E. & Sakmann, B. (1995). Fractional calcium currents through recombinant GluR channels of the NMDA, AMPA and kainate receptor subtypes. *Journal of Physiology* **485**, 403–418.

Colquhoun, D., Jonas, P. & Sakmann, B. (1992). Action of brief pulses of glutamate on AMPA/kainate receptors in patches from different neurones of rat hippocampal slices. *Journal of Physiology* **458**, 261–287.

Franke, Ch., Hatt, H. & Dudel, J. (1987). Liquid filament switch for ultra-fast exchanges of solutions at excised patches of synaptic membrane of crayfish muscle. *Neuroscience Letters* **77**, 199–204.

Gulyás, A. I., Miles, R., Sík, A., Tóth, K., Tamamaki, N. & Freund, T. F. (1993). Hippocampal pyramidal cells excite inhibitory neurons through a single release site. *Nature* **366**, 683–687.

Han, Z.-S., Buhl, E. H., Lörinczi, Z. & Somogyi, P. (1993). A high degree of spatial selectivity in the axonal and dendritic domains of physiologically identified local-circuit neurons in the dentate gyrus of the rat hippocampus. *European Journal of Neuroscience* **5**, 395–410.

Hestrin, S. (1993). Different glutamate receptor channels mediate fast excitatory synaptic currents in inhibitory and excitatory cortical neurons. *Neuron* **11**, 1083–1091.

Hollmann, M., Hartley, M. & Heinemann, S. (1991). Ca^{2+} permeability of KA–AMPA-gated glutamate receptor channels depends on subunit composition. *Science* **252**, 851–853.

Hou, T.-T., Johnson, J. D. & Rall, J. A. (1991). Parvalbumin content and Ca^{2+} and Mg^{2+} dissociation rates correlated with changes in relaxation rate of frog muscle fibres. *Journal of Physiology* **441**, 285–304.

Iino, M., Ozawa, S. & Tsuzuki, K. (1990). Permeation of calcium through excitatory amino acid receptor channels in cultured rat hippocampal neurones. *Journal of Physiology* **424**, 151–165.

Jonas, P., Major, G. & Sakmann, B. (1993). Quantal components of unitary EPSCs at the mossy fibre synapse on CA3 pyramidal cells of rat hippocampus. *Journal of Physiology* **472**, 615–663.

Jonas, P., Racca, C., Sakmann, B., Seeburg, P. H. & Monyer, H. (1994). Differences in Ca^{2+} permeability of AMPA-type glutamate receptor channels in neocortical neurons caused by differential GluR-B subunit expression. *Neuron* **12**, 1281–1289.

Jonas, P. & Sakmann, B. (1992). Glutamate receptor channels in isolated patches from CA1 and CA3 pyramidal cells of rat hippocampal slices. *Journal of Physiology* **455**, 143–171.

Jonas, P. & Spruston, N. (1994). Mechanisms shaping glutamate-mediated excitatory postsynaptic currents in the CNS. *Current Opinion in Neurobiology* **4**, 366–372.

Lerma, J., Morales, M., Ibarz, J. M. & Somohano, F. (1994). Rectification properties and Ca^{2+} permeability of glutamate receptor channels in hippocampal cells. *European Journal of Neuroscience* **6**, 1080–1088.

Lerma, J., Paternain, A. V., Naranjo, J. R. & Mellström, B. (1993). Functional kainate-selective glutamate receptors in cultured hippocampal neurons. *Proceedings of the National Academy of Sciences of the USA* **90**, 11688–11692.

Levitan, E. S. & Kramer, R. H. (1990). Neuropeptide modulation of single calcium and potassium channels detected with a new patch clamp configuration. *Nature* **348**, 545–547.

Lewis, C. A. (1979). Ion-concentration dependence of the reversal potential and the single channel conductance of ion channels at the frog neuromuscular junction. *Journal of Physiology* **286**, 417–445.

Livsey, C. T., Costa, E. & Vicini, S. (1993). Glutamate-activated currents in outside-out patches from spiny *versus* aspiny hilar neurons of rat hippocampal slices. *Journal of Neuroscience* **13**, 5324–5333.

Livsey, C. T. & Vicini, S. (1992). Slower spontaneous excitatory postsynaptic currents in spiny *versus* aspiny hilar neurons. *Neuron* **8**, 745–755.

McBain, C. J. & Dingledine, R. (1993). Heterogeneity of synaptic glutamate receptors on CA3 stratum radiatum interneurones of rat hippocampus. *Journal of Physiology* **462**, 373–392.

Mayer, M. L. & Westbrook, G. L. (1987). Permeation and block of *N*-methyl-D-aspartic acid receptor channels by divalent cations in mouse cultured central neurones. *Journal of Physiology* **394**, 501–527.

Partin, K. M., Patneau, D. K., Winters, C. A., Mayer, M. L. & Buonanno, A. (1993). Selective modulation of desensitization at AMPA *versus* kainate receptors by cyclothiazide and concanavalin A. *Neuron* **11**, 1069–1082.

Patneau, D. K. & Mayer, M. L. (1991). Kinetic analysis of interactions between kainate and AMPA: Evidence for activation of a single receptor in mouse hippocampal neurons. *Neuron* **6**, 785–798.

Patneau, D. K., Vyklicky, L. & Mayer, M. L. (1993). Hippocampal neurons exhibit cyclothiazide-sensitive rapidly desensitizing responses to kainate. *Journal of Neuroscience* **13**, 3496–3509.

Ribak, C. E., Nitsch, R. & Seress, L. (1990). Proportion of parvalbumin-positive basket cells in the GABAergic innervation of pyramidal and granule cells of the rat hippocampal formation. *Journal of Comparative Neurology* **300**, 449–461.

Ribak, C. E. & Seress, L. (1983). Five types of basket cell in the hippocampal dentate gyrus: a combined Golgi and electron microscopic study. *Journal of Neurocytology* **12**, 577–597.

Robinson, R. A. & Stokes, R. H. (1965). *Electrolyte Solutions.* Butterworths, London.

Schneggenburger, R., Zhou, Z., Konnerth, A. & Neher, E. (1993). Fractional contribution of calcium to the cation current through glutamate receptor channels. *Neuron* **11**, 133–143.

Schwartzkroin, P. A. & Mathers, L. H. (1978). Physiological and morphological identification of a nonpyramidal hippocampal cell type. *Brain Research* **157**, 1–10.

Seress, L. & Ribak, C. E. (1983). GABAergic cells in the dentate gyrus appear to be local circuit and projection neurons. *Experimental Brain Research* **50**, 173–182.

Silver, R. A., Colquhoun, D., Cull-Candy, S. G. & Edmonds, B. (1994). Mechanisms underlying decay of the fast component of EPSCs in rat cerebellar granule cells. *Journal of Physiology* **476**, 67*P*.

Sloviter, R. S. (1991). Permanently altered hippocampal structure, excitability, and inhibition after experimental status epilepticus in the rat: The 'dormant basket cell' hypothesis and its possible relevance to temporal lobe epilepsy. *Hippocampus* **1**, 41–66.

Soriano, E. & Frotscher, M. (1993). GABAergic innervation of the rat fascia dentata: a novel type of interneuron in the granule cell layer with extensive axonal arborization in the molecular layer. *Journal of Comparative Neurology* **334**, 385–396.

Spruston, N., Jonas, P. & Sakmann, B. (1995). Dendritic glutamate receptor channels in rat hippocampal CA3 and CA1 pyramidal neurons. *Journal of Physiology* **482**, 325–352.

Stuart, G. J., Dodt, H.-U. & Sakmann, B. (1993). Patch-clamp recordings from the soma and dendrites of neurons in brain slices using infrared video microscopy. *Pflügers Archiv* **423**, 511–518.

Trussell, L. O., Zhang, S. & Raman, I. M. (1993). Desensitization of AMPA receptors upon multiquantal neurotransmitter release. *Neuron* **10**, 1185–1196.

WISDEN, W. & SEEBURG, P. H. (1993). Mammalian ionotropic glutamate receptors. *Current Opinion in Neurobiology* **3**, 291–298.

WOODHULL, A. M. (1973). Ionic blockage of sodium channels in nerve. *Journal of General Physiology* **61**, 687–708.

WYLLIE, D. J. A. & CULL-CANDY, S. G. (1994). A comparison of non-NMDA receptor channels in type-2 astrocytes and granule cells from rat cerebellum. *Journal of Physiology* **475**, 95–114.

Acknowledgements

We thank Drs M. Häusser and H. Markram for critically reading the manuscript and M. Kaiser for technical assistance. Supported by the Deutsche Forschungsgemeinschaft (SFB-317/B14 grant to P.J. and a Graduiertenkolleg-Stipendium to J.R.P.G.).

Author's present address

P. Jonas: Physiologisches Institut der Technischen Universität, Biedersteiner Straße 29, 80802 München, Germany.

Received 3 August 1994; accepted 1 November 1994.